Universidad del País Vasco
Euskal Herriko Unibertsitatea

ZTF-FCT
Zientzia eta Teknologia Fakultatea
Facultad de Ciencia y Tecnología

End-of-degree Project

Degree in Chemistry

# STUDY OF MONODIMENSIONAL COMPOUNDS BASED ON GROUP 6 TETRAOXOMETALATES WITH Cu(CYCLAM) COMPLEXES

Author:
ESTIBALIZ RUIZ BILBAO
Supervisors:
*JUAN MANUEL GUTIERREZ-ZORRILLA*
*BEÑAT ARTETXE*

Leioa, 27 June 2016

# TRABAJO FIN DE GRADO
# GRADO EN QUIMICA

# STUDY OF MONODIMENSIONAL COMPOUNDS BASED ON GROUP 6 TETRAOXOMETALATES WITH Cu(CYCLAM) COMPLEXES

**MEMORIA PRESENTADA POR ESTIBALIZ RUIZ BILBAO**

**FECHA DE MATRICULACIÓN Y DEFENSA:** JUNIO-JULIO 2016

**DIRECTORES:** JUAN MANUEL GUTIÉRREZ-ZORRILLA
BEÑAT ARTETXE

**DEPARTAMENTO:** QUÍMICA INORGÁNICA

## TABLE OF CONTENTS

# 1. INTRODUCTION

## 1.1. POLYOXOMETALATES

Polyoxometalates (POMs) are anionic clusters formed by the combination between oxygen and early transition metals (e.g.: V, Nb, Ta, Mo, W) at their highest oxidation states.[1] POMs are well-known due to their remarkable structural and magnetic properties and also for their applications in catalysis and medicine.[2,3] Structurally, classical POMs are formed by the condensation of polyhedral $MO_x$ units with a coordination of metals between 4 and 7 and commonly showing an octahedral structure.

The POM formation equilibria in aqueous solutions is determined by multiple factors: pH and ionic strength of the medium, concentration of precursors, temperature and pressure, and even the type of counterion employed.[4,5] In inorganic chemistry, there has been a big interest in the aqueous solution of POMs because a wide variety of discrete molecules, ranging in complexity, can be obtained depending on the pH value.[6]

It is unknown that polynuclear species are formed at a pH higher than 10. Correspondingly, at an alkali pH, instead of POMs, discrete oxyanions are observed. An acidification of the oxyanion solution results in condensation and the formation of larger polynuclear compounds such as POMs,[4] except for vanadium, where polymeric species are observed at a pH higher than 10, and the discrete oxyanion, $VO_4^{3-}$, is only observed at pH higher than 13.[7-10]

The following Figure 1 shows the different predominant species in aqueous solution, at different pH, for the transition metals of the group 6, Cr, Mo and W. It can be seen that in an alkali pH, the predominant specie, for the three metals, is the oxyanion $[MO_4]^{2-}$, while at a more acidic pH the predominant species are larger polynuclear compounds.[11-14]

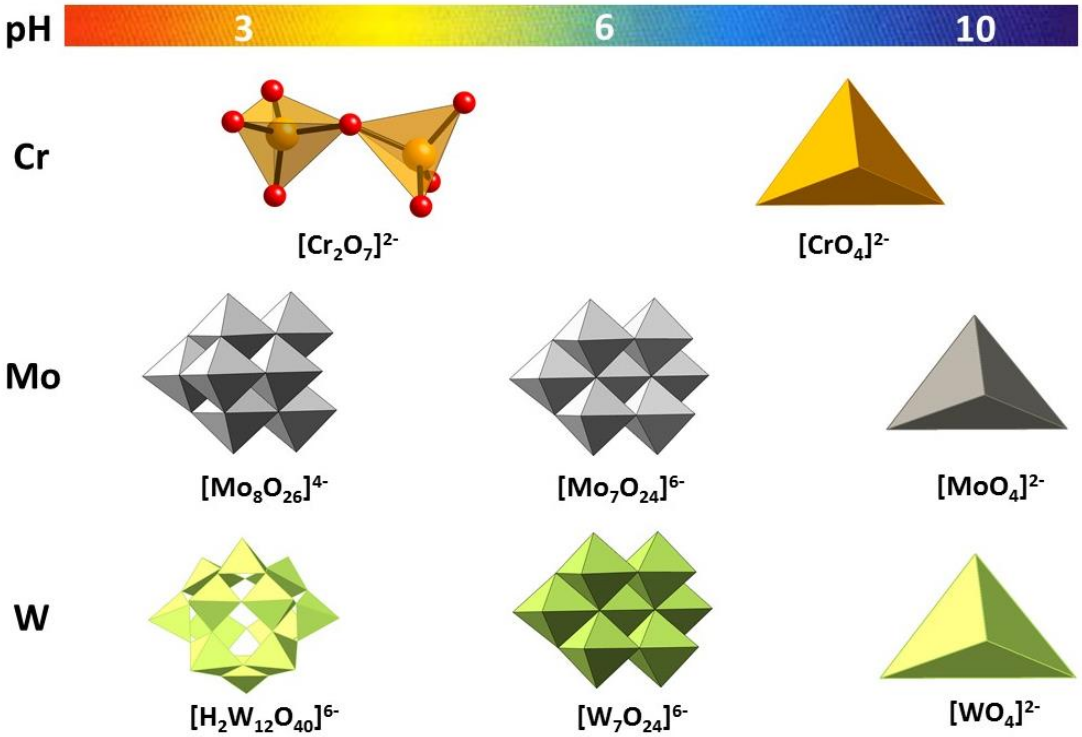


*Figure 1.- Predominant species and structures for the transition metals of the group 6 (Cr, Mo and W) at different pH.*

### 1.2. OXYANIONS

Oxyanions, or oxo anions, with the formula $[MO_x]^{y-}$ can be assembled from a Lewis acid plus some oxide ions, $O^{2-}$, as Lewis bases.

When we deal with some elements in positive oxidation states in aqueous solution, we are not dealing with cations, but with species such as oxides or hydroxides, which may react as weak oxo acids or finally as strong oxo acids, ionizing completely to hydronium ions and **oxo anions**, $[MO_x]^{y-}$.

Table 1 shows the oxyanions of metals whose oxidation state matches with their group number. This work will be focused on oxyanion of group 6 transition metals, Cr, Mo and W, whose oxyanion formula can be seen in Table 1.[15]

*Table 1.- Oxyanions in which the central atom oxidation state equals the group number.*

| | 13/III | 14/IV | 15/V | 16/VI | 17/VII | 18/VIII |
|---|---|---|---|---|---|---|
| **Block p** | $BO_3^{3-}$ Borate | $CO_3^{2-}$ Carbonate | $NO_3^-$ Nitrate | | | |
| | $AlO_4^{5-}$ Aluminate | $SiO_4^{4-}$ Silicate | $PO_4^{3-}$ Phosphate | $SO_4^{2-}$ Sulfate | $ClO_4^-$ Perchlorate | |
| | $GaO_4^{5-}$ Gallate | $GeO_4^{4-}$ Germanate | $AsO_4^{3-}$ Arsenate | $SeO_4^{2-}$ Selenate | $BrO_4^-$ Perbromate | |
| | | $SnO_6^{8-}$ Stannate | $SbO_6^{7-}$ Antimoniate | $TeO_6^{6-}$ Tellurate | $IO_6^{5-}$ Periodate | $XeO_6^{4-}$ Perxenate |
| | | $PbO_6^{8-}$ Plumbate | | | | |
| **Block d** | | | $VO_4^{3-}$ Vanadate | $CrO_4^{2-}$ Chromate | $MnO_4^-$ Permanganate | |
| | | | | $MoO_4^{2-}$ Molybdate | $TcO_4^-$ Pertechnetate | |
| | | | | $WO_4^{2-}$ Wolframate | $ReO_4^-$ Perrhenate | $OsO_6^{4-}$ Perosmate |

### 1.3. OXYANIONS OF GROUP 6 TRANSITION METALS

As previously mentioned (Table 1), the molecular formulas for oxyanions of the early transition metals of the group 6 are $CrO_4^{2-}$, $MoO_4^{2-}$ and $WO_4^{2-}$, respectively, in where each metal has VI oxidation state. These ions present a tetrahedral structure in which the metal is surrounded by four oxygen atoms which are directed toward the corners of a regular tetrahedron (Figure 2).

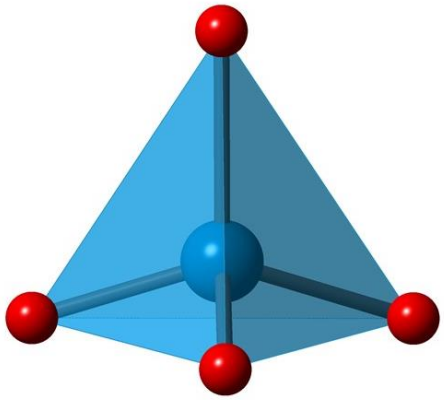

| Metal | M-O (Å) | O-M-O (°) |
|---|---|---|
| Cr | 1.641 | 109.4 |
| Mo | 1.765 | 109.5 |
| W | 1.776 | 109.5 |

*Figure 2.- Tetrahedral structure of an oxyanion and the average M-O distances and O-M-O angles for the transition metals of the group 6.*

Cr(VI), Mo(VI) and W(VI) have $d^0$ configuration. Due to the extensive polarization of the anions, compounds with a VI oxidation state are highly covalent and they can stablish some M-O bonds with π character.

Due to a small increase in successive ionization energies, most of the transition metals have multiple oxidation states. High ionization states become progressively less stable for the elements on the right side of the d-block. The stability of the higher oxidation states progressively increases going down the group. Because of that, molybdenum and tungsten with a high oxidation state of VI are very stable, more than chromium with the same oxidation state. This can be seen in the fact that the oxyanion $[CrO_4]^{2-}$ is a powerful oxidant, whereas the tungstate ion or molybdate oxyanions are extremely stable and have no tendency to act as oxidants.[16]

The high stability of Cr(III) can be explained by the Frost diagram (Figure 3). Cr(III) in basic media forms the chromium hydroxide, $Cr(OH)_3$, which is the most stable specie for chromium, with no tendency to be neither reduced nor oxidized. The Frost diagram also shows that although Mo(IV) is the most stable specie for molybdenum, Mo(VI) also present a high stability. Finally, it can be seen that W(VI) is the specie of tungstate than present a highest stability.

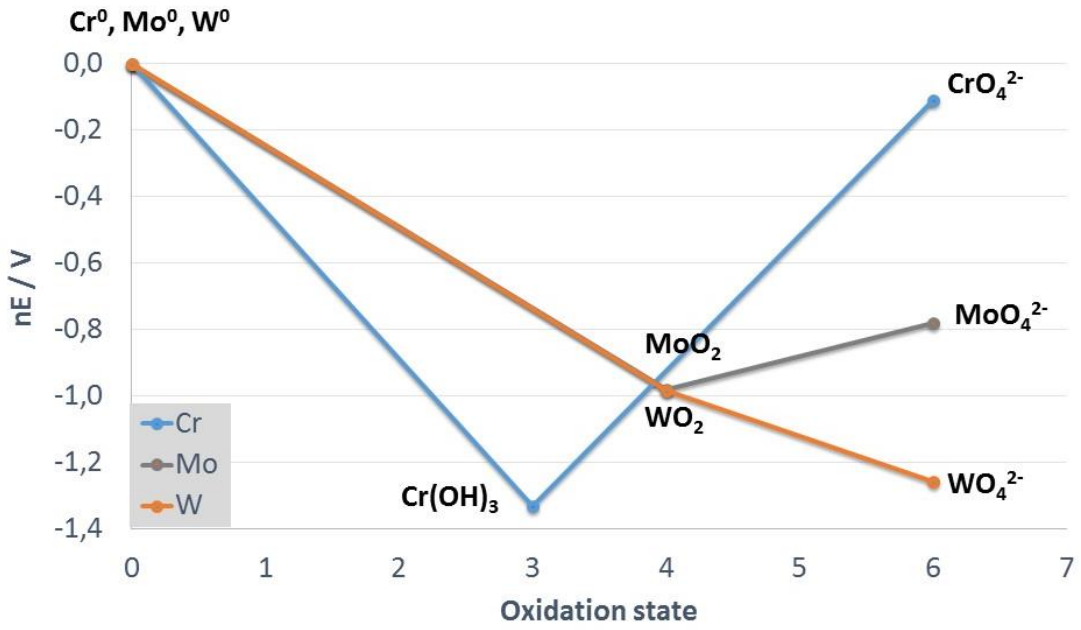


*Figure 3.- Frost diagram for the group 6 transition metals Cr, Mo and W in basic media.*

Cr, Mo and W are transition metals from the group 6 so they have a total of six valence electrons, resulting in a maximum oxidation state of +6. Nevertheless, as previously said, Cr(VI) is not as stable as Mo(VI) and W(VI), and this is due to the suitable charge-to-radius ratio that the latter have. The three metals have the same charge but their sizes are different. Cr is in the period 4 so it is smaller than Mo, period 5, and W, period 6. However, W has not a higher radius than Mo but they share similar size due to relativistic effects (Figure 4).

Relativistic effects are explained by Dirac, which is a modification of the Schrödinger equation which also describes how the wave function of a physical system evolves with the time. Solution of Dirac equation that do incorporate relativity theory show that both the radial and the angular parts of the wave functions for the heavier atoms, sixth row, in the periodic table are appreciably altered by relativistic effects.[17,18]

The radial effect is known as relativistic contraction. We can think of the electron as a particle that is accelerated to a certain radial velocity by the attraction of the nucleus so that, the more the nuclear charge builds up, the more the radial velocity, v, builds up too (Eq. 1).

$$v = \frac{e^2 Z}{4\pi\varepsilon_0 \hbar} \qquad (\boldsymbol{Eq.\,1})$$

This velocity increases until it may begin to approach the speed of light, which can be expressed in units of atomic charge as 137.036 atomic unit. This way, the average radial velocity of 1s electron of an atom is equal to the nuclear charge of that atom, Z, (Eq. 2):

$$Radial\ velocity = \frac{Z}{137.036} \qquad (\boldsymbol{Eq.\,2})$$

According to Einstein's theory of relativity, the mass, m, of a particle increases over its rest mass, $m_0$, when its speed, v, approaches the speed of light, c (Eq. 3):

$$m = \frac{m_0}{\sqrt{\left(1 - \left(\frac{v}{c}\right)^2\right)}} \qquad (\boldsymbol{Eq.\,3})$$

On the contrary, the radius of the Bohr orbit of an electron is inversely proportional to both the mass of the electron and its nuclear charge. Thus, the higher the velocity of an electron and nuclear charge of an atom, the higher its mass and the smaller its Bohr radius if comparing with the one expected (Eq. 4):

$$r = \frac{n^2 \hbar^2 4\pi\varepsilon_0}{m_e Z e^2} \qquad (\boldsymbol{Eq.4})$$

Hence, as the W, in the sixth row in the periodic table, has a high nuclear charge, it is affected by relativistic contraction and its radius is smaller than the expected one from its position in the periodic table.

The relativistic effects also affect the 2s and higher s orbitals roughly as much because of their inner lobes, which are close to the highly charged nucleus. Relativistic effect is present to a lesser extent among p orbitals and is almost absent among d and f orbitals.

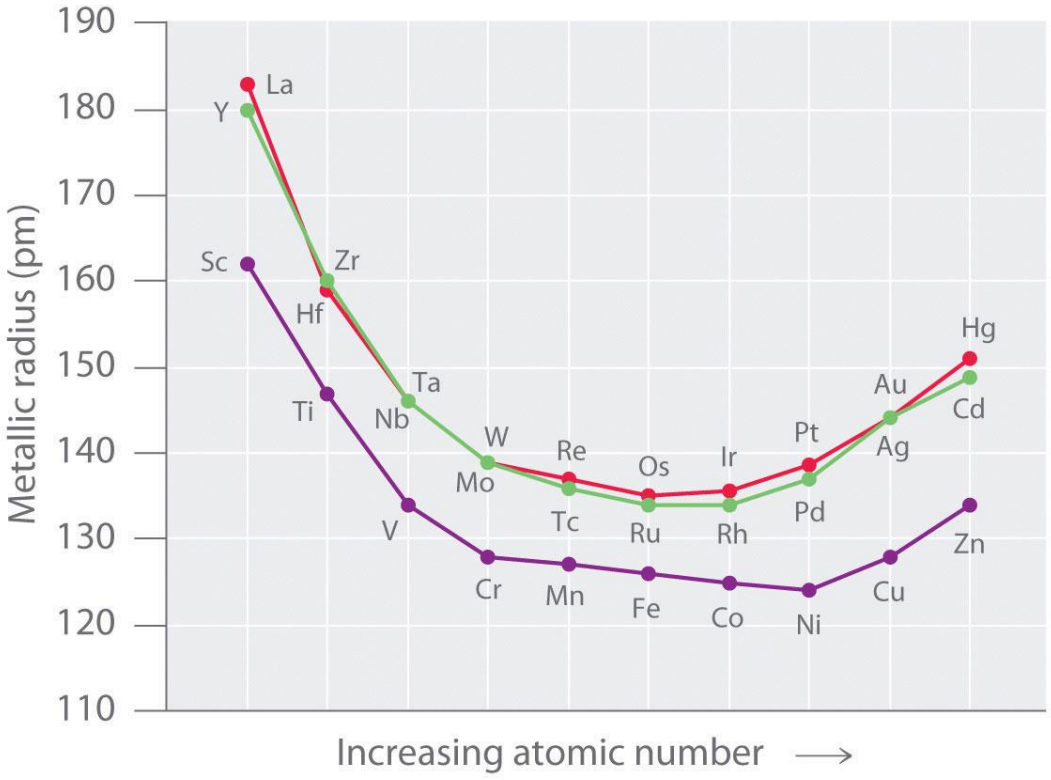


*Figure 4.- Representation of the metallic radius of the transition metals.*

### 1.3.1. Synthesis of chromate, molybdate and tungstate anions

Chromium is found in nature mainly as chromite, which is an iron (II) dichromate ($FeCr_2O_4$) mineral which can also be found with magnesium substituting the iron. Chromate and dichromate coexist in a chemical equilibrium which is pH dependant.

$$2\ CrO_4^{2-}(aq) + 2\ H^+(aq) \leftrightarrow\ Cr_2O_7^{2-}(aq) +\ H_2O(l)$$

Hence, if shifting this equilibrium to the left, by adjusting the pH, the chromate is obtained, which can be obtained as a chromium salt by precipitating with a metal.

Molybdenum was successfully isolated for the first time by the Swedish chemist Peter Jacob Hjelm in 1782.[19] Molybdenum is not found free in nature. For this early transition metal, the chief ore is molybdenite or molybdenum disulphide, $MoS_2$, but molybdates such as lead molybdate, $PbMoO_4$ (wulfenite) and calcium molybdate, $CaMoO_4$, are also found.[13] The mineral is usually roasted in an excess of air to yield molybdenum trioxide ($MoO_3$), which, after purification, can be reduced with hydrogen to the metal Mo. For obtaining molybdate, $MoO_3$ reacts at high temperatures with various metal oxides to form the corresponding molybdates. Another way of obtaining molybdates is by dissolving $MoO_3$ in alkali aqueous solution and crystallizing the formed molybdate as a salt.[20]

Tungsten, or wolfram, metal was first isolated in 1783 by the Spanish chemist and mineralogists Juan José and Fausto Elhuyar, by the reduction of the tungsten oxide, derived from the mineral wolframite[21]. Tungsten, as molybdenum, is not found in nature as a free metal. Although tungsten occurs as tungstenite or tungsten disulphide, $WS_2$, the most important ores of this metal are tungstates such as scheelite or calcium tungstate, $CaWO_4$, stolzite or lead tungstate, $PbWO_4$ and wolframite, which is an iron and/or manganese mineral with the formula $Fe(Mn)WO_4$ [13,22]. Appart from the scheelite or stilzite, the tungstate can be also obtained from the same two ways as molybdenum.

### 1.3.2. Applications of chromate, molybdate and tungstate

Chromates, molybdates and tungstates have a wide range of applications. Some applications are common for the three of them:

- **Catalysis**. Nickel chromate and molybdate have been used as aromatization catalysts for hydrocarbons. The chromate has been also used to dehydrogenate and cyclize paraffin hydrocarbons and to selectively hydrogenate butadiene to butylene in the gas phase.[23]

Molybdenum and tungsten complexes are also well-known catalyst for many reactions. Molybdate ions participate in the selective oxidation of, for example, propene, ammonia, and air to acrylonitrile, acetonitrile and other chemicals which are raw materials for the plastics and fibre industries. Cobalt and nickel molybdates are also used as catalysts with applications for hydrodesulphurisation[24]. It should be highlighted the use of iron molybdate as catalyst for the obtaining of formaldehyde by the oxidation reaction of methanol.

As molybdates, tungstates can also be used as catalysts in the oxidation of methanol for obtaining formaldehyde, however, the effect of the tungsten has been proved to be 20 times less than the one for molybdate.[25]

- **Pigments**. Chromate and molybdate-based pigments are used for two properties: stable colour formation and corrosion inhibition. For example, zinc chromate and molybdate are the basis of corrosion inhibiting pigments which are used as primer paints.[26]

Barium, calcium, cadmium, cobalt and lead and zinc tungstates are also widely used as bright white pigments.[27]

There are other applications that are specific for molybdates or tungstates:

- **Corrosion inhibitors.** Sodium molybdate has been used for many years as a substitute for chromates for the inhibitions of corrosion in mild steels over a wide range of pH. Molybdates have a very low toxicity and are less aggressive oxidants than chromates toward organic additives that may be used in corrosion inhibiting

formulation.[28,29] A prime application is in cooling water in air-conditioning and heating systems to protect mild steel used in their construction.

Molybdates are used to inhibit corrosion in water-based hydraulic systems and in automobile engine anti-freezing. Molybdate solutions protect against rusting of steel parts during machining.

Corrosion inhibiting pigments, primarily zinc molybdate, but also molybdates of calcium and strontium, are used commercially in paints. These pigments are white and can be used as a primer or as a tint with any other colour.[29]

- **In agriculture.** Molybdenum is an essential trace element for plants and animals as it is an essential component of the enzyme nitrogenase (Figure 5) which catalyses the conversion of atmospheric nitrogen to ammonia. Accordingly, molybdate is applies in fertiliser formulations.[30]

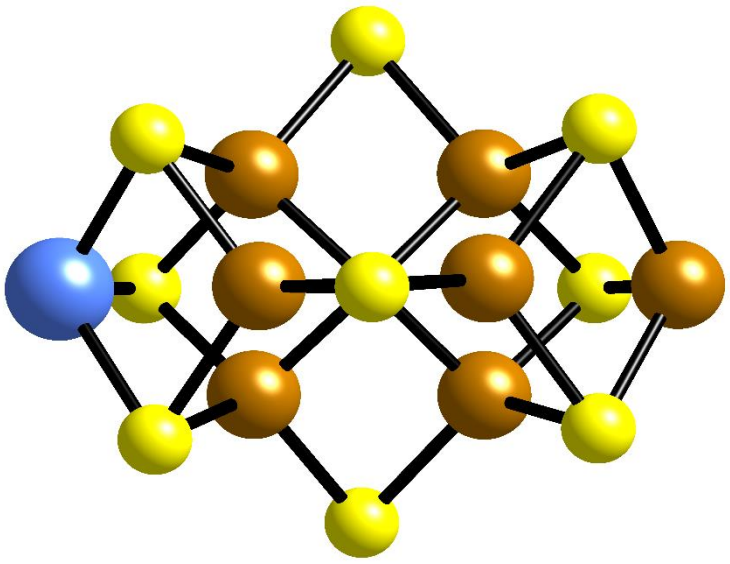

*Figure 5.- Nitrogenase active-centre with Mo atom in blue.*

- **Mining and mineral separation.** There are several tungstate compounds (Na, Li) that are used as safe and effective alternatives to traditional organic heavy liquids.[31]
- **Oxidant**. Both chromate and dichromate, with Cr(VI), act as good oxidants as they reduce their oxidation state from Cr(VI) to Cr(III).[32]
- **Medicine.**[33] Although it is still not widely used in medicine, the chemistry of molybdenum (VI) oxo-complexes have been intensively investigated because of their

high importance in biochemical applications. Mo(VI) oxo-complexes have been proved to promote selective cleavage of peptides and proteins. This can be widely used in the study of protein function and solution structure, mapping of enzyme active sites and conformational changes.[12] The interest in complexes of Mo(VI) is partly due to the fact that molybdenum is an essential element in various biological systems, of particular interest is the role of molybdenum (VI) in the fixation of nitrogen by some bacteria commonly associated with legumes.[34]

Molybdates in aqueous solutions are of special interest due to the implication of Mo(VI) and (V) in some important enzymatic redox systems. Most such complexes are labile, potentials for changing oxidation states are low, and the tendency to form O- and S- bridged polynuclear complexes in high. These properties make Mo a versatile site for reaction and catalysis in biochemical systems.[11]

Tungstates also have medical applications, although they are in **dental medicine**. Known tungsten compounds in dental composites are sodium tungstate, potassium tungstate, manganese tungstate, calcium tungstate, strontium tungstate and barium tungstate. These various tungstates are added to give good definition in the dental X-rays.

Chromate, unlike molybdates and tungstates is not used in medicine because Cr(VI) is a carcinogenic and mutagenic agent. $CrO_4^{2-}$ is isostructural with the sulfate ion ($SO_4^{2-}$). Sulfate transport proteins in the body, so proteins uptake chromate, which damages DNA.[35,36]

### 1.4. COPPER-*CYCLAM* COMPLEX

Copper complexation is currently attracting a huge amount of research interest owing to the importance of the complexes of $Cu^{2+}$ in numerous fields between those it should be highlighted biology, pharmaceutic and medicine. A high concentration of copper in the body is known to be potentially toxic, causing damage to lipids, proteins and DNA, which derivates on serious diseases, such as Wilson desease.[37,38] However, the essentiality of copper ions in biological systems has long been recognized. Copper

ions are integrated components of some critical protein structures, involved in catalytic activities and crucial for regulatory functions.[39] Indeed, significant progress has been achieved in the past years in nuclear medicine to find stable chelates of radioactive copper ions, particularly $^{64}Cu$ and $^{67}Cu$. Therefore, complexes of $Cu^{2+}$ suitable for use as radiopharmaceuticals must be thermodynamically stable and kinetically inert in the highly competitive biological media.[40]

Tetraazamacrocycles, such as *cyclam*, also continue to attract the interest of organic, inorganic and biochemists owing to their ability to form complexes with very high thermodynamic, kinetic and electrochemical stability with respect to metal dissociation.[41]

1, 4, 8, 11-tetraazacyclotetradecane (Figure 6), commonly known as *cyclam*, is a well-known macrocyclic ligand with four secondary amines that forms highly stable complexes with virtually/almost all transition metal ions.

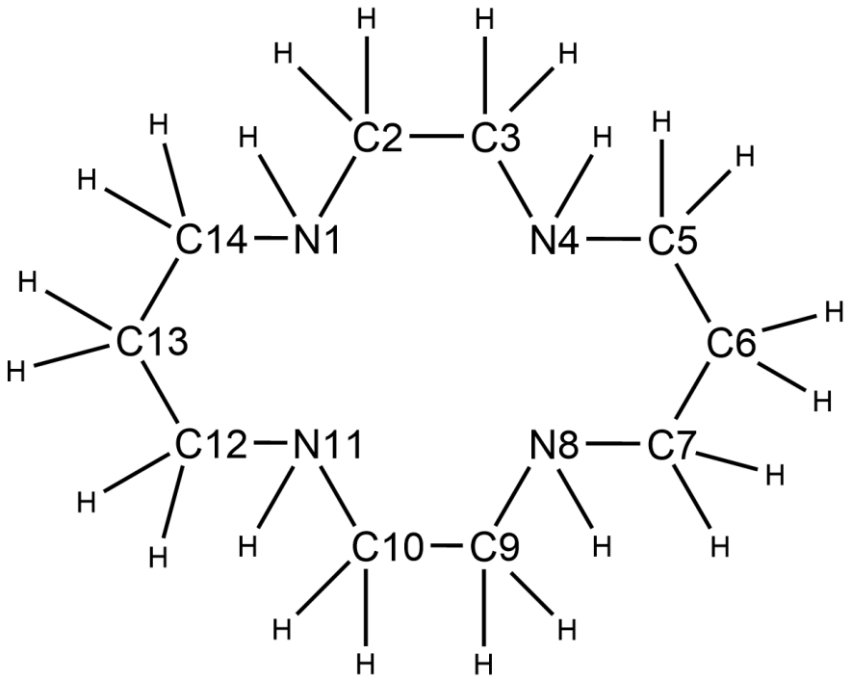


*Figure 6.- 1,4,8,11-tetraazacyclotetradecane molecule.*

There are five possible geometrical isomers for *cyclam* depending on its configuration (Figure 7).[42]

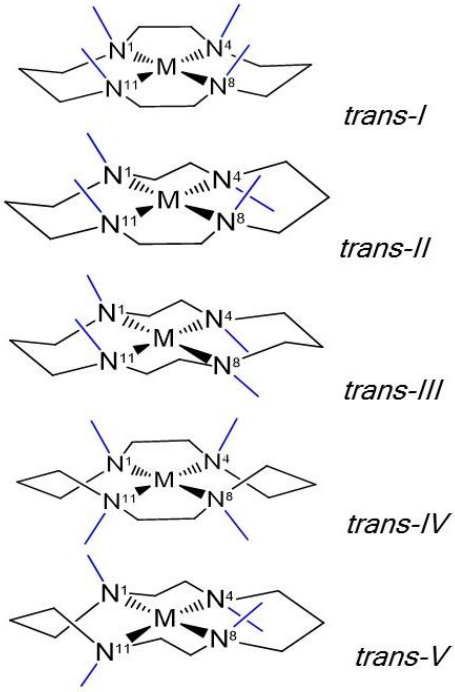


*Figure 7.- The five possible configurations for the cyclam ligand.*

*Cyclam* is currently being used in many biomedical areas, including biomimetics, anti-human immunodeficiency virus (HIV) agents by blocking the entry of HIV into cells, radioactive diagnosis and treatment of cancer, magnetic resonance imaging (MRI) contrast agents and Positron Emission Tomography (PET).[43,44]

These potential and versatile applications are stimulating researches to exploit new *cyclam* based ligands and complexes with potential chemical, biological and catalytic properties. Thus, nowadays, copper-*cyclam* complex is being investigated as both copper and *cyclam* present anticancer properties. The use of Cu(*cyclam*) instead of other chemotherapy, cause fewer side effects.[45] In addition, copper-*cyclam* complexes are soluble in water, which is highly required for biomedical applications.[41,46]

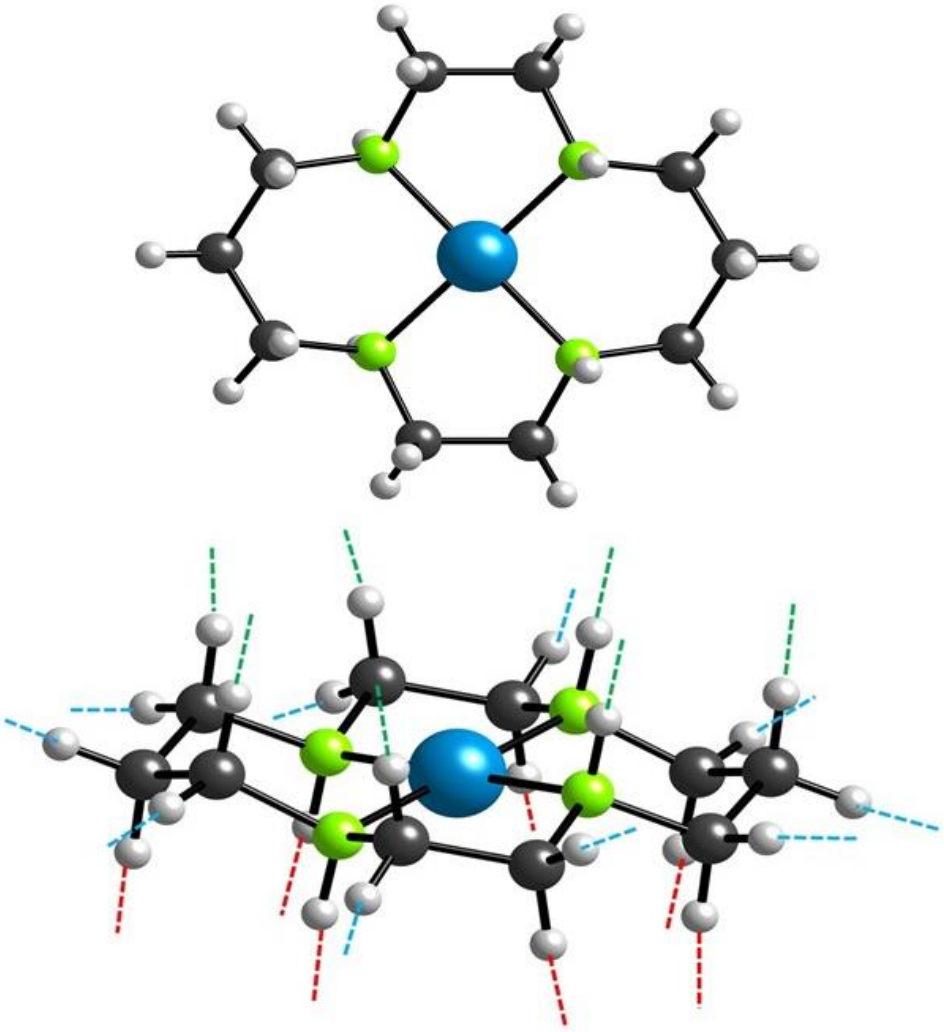

*Figure 8.- Top and side views of Cu(cyclam) complex, with the indications of potential hydrogen bonds.*

The lateral view of Cu(*cyclam*) (Figure 8) shows the different type of hydrogen bonds that can be formed by *cyclam* ligand. Molecular formula of *cyclam* is $C_{10}H_{24}N_4$, so that it can form 24 H-bonds, 4 N-H···X and 20 C-H···X bonds. The 4 hydrogen atoms of the secondary amines, -NH-, are located 2 at the top and the other 2 at the bottom. The other 20 hydrogen atoms are forming $-CH_2$ bonds, and are located in axial and equatorial so that 5 hydrogens are located at the top, other 5 at the bottom and the remaining 10 hydrogens are located in the laterals. This way, *cyclam* can form 7 hydrogen bonds in the upper part (green), other 7 hydrogen bonds at the bottom (red) and 10 hydrogen bonds in the laterals (blue). This possibility of forming so many hydrogen bonds confer to *cyclam* the ability of forming high stable complexes.

## 1.5. MAIN OBJECTIVES

This work fits within one of the research lines of *Departamento de Química Inorgánica de la Facultad de Ciencia y Tecnología de la Universidad del País Vasco UPV/EHU*. This research consists in the synthesis and structural characterization of organic-inorganic hybrid compounds based on interaction between oxyanions and metal-organic complexes, and its main objectives are to combine both type of components in quest of new properties or structural motifs to enrich the field of coordination chemistry. The synthesis of these hybrid compounds could report new compounds, with new properties and reactivities.

The main objective of this research is **to carry out a comparative study of the [Cu(cyclam)]$MO_4 \cdot nH_2O$ complexes with group 6 transition metals and see how the presence of the oxyanion affects to the structure, crystal packing and magnetic properties.**

Some metal-organic ligands have shown interesting properties in several areas mentioned above. This is the example of Cu(*cyclam*) which is of great interest in chemical and biochemical fields mainly because of its anticancer properties.

From the transition metals of the group 6, molybdenum is the only one that shows to have anticancer properties. Thus, a complex with Cu(*cyclam*) and molybdate, such as [Cu(cyclam)][$MoO_4$] (**Compound 2**), can be of great interest in the field of chemistry and medicine, as it had been previously seen.

On the other hand, the study of the oxometalates with chromium and tungsten with Cu(cyclam); [Cu(cyclam)][$CrO_4$] (**Compound 1**) and [Cu(cyclam)][$WO_4$] (**Compound 3**), are also of big interest to study how the structure of these compounds varies along the group 6.

# 2. EXPERIMENTAL SECTION

## 2.1. MATERIALS AND METHODS

In this section the techniques and experimental conditions employed for the synthesis and characterization of the compounds $[Cu(C_{10}H_{24}N_4)][CrO_4]\cdot 3H_2O$ (**1**), $[Cu(C_{10}H_{24}N_4)][MoO_4]\cdot 4H_2O$ (**2**) and $[Cu(C_{10}H_{24}N_4)][WO_4]\cdot 5.5H_2O$ (**3**) are described. The Fourier-Transform Infrared (FT-IR) measurements were done in the Department of Inorganic Chemistry. X-ray, elemental analysis and Electron Paramagnetic Resonance (EPR) analysis were done in the General Research Services (SGIker) of the University of the Basque Country UPV/EHU. All the chemicals used in the synthesis procedure were obtained from commercial sources and used without further purification.

Elemental analysis of carbon, hydrogen and nitrogen were determined on a Perkin-Elmer 240 CHN analyser. Fourier Transform Infrared (FT-IR) spectra were obtained as KBr pellets on a SHIMADZU FTIR-8400S spectrometer. The spectra were done with 4 $cm^{-1}$ resolution and in a wavenumber range between 400 and 4000 $cm^{-1}$, using IRSolutions software for data processing. Electron paramagnetic resonance (EPR) spectra were recorded on Bruker ELEXSYS 500 (superhigh-Q resonator ER-4123-SHQ) and Bruker EMX (ER-510-QT resonator) continuous wave spectrometers for Q- and X-bands, respectively (magnetic calibration: NMR probe; frequency inside the cavity determined with microwave counter).

## 2.2. SYNTHESIS PROCEDURE

The same synthetic procedure was carried out for obtaining compounds **1**, **2** and **3**:

To a solution of a transition metal salt of group 6 (0.7 mmol) in distilled water (15 mL) was added, dropwise, another solution of $CuSO_4\cdot 5H_2O$ (0.075g, 0.3 mmol) and 1,4,8,11-tetraazacyclotetradecane (*cyclam*) (0.040g, 0.2 mmol) in distilled water (15 mL). The pH of the mixture was adjusted to 10 by the addition of NaOH (0.1 M). After 1 hour of stirring at room temperature, the solution was filtered and poured in a crystallizer. Crystals appeared in two weeks at the bottom of the crystallizer.

**Synthesis of $[Cu(C_{10}H_{24}N_4)][CrO_4]\cdot 3H_2O$ (1)**

The transition metal source used was $K_2Cr_2O_7$ (0.103 g, 0.35 mmol). The obtained crystals were brown. Yield: 35 mg, 40%. Anal. Calc. (found) (%): C, 27.68 (24.59); H, 6.97 (5.96); N, 12.91 (11.35). IR ($cm^{-1}$, KBr pellet): 3448 (vs), 3229 (m), 3165 (s), 2936 (m), 2864 (m), ≈1630 (w), 1473 (w), 1451 (w), 1429 (w), 1105 (m), 1071 (w), 1062 (w), 1016 (m), 1009 (m), 962 (s), 883 (s), 440 (w).

**Synthesis of $[Cu(C_{10}H_{24}N_4)][MoO_4]\cdot 4H_2O$ (2)**

The transition metal source used was $NaMoO_4\cdot 2H_2O$ (0.169 g, 0.7 mmol). The obtained crystals were purple. Yield: 29 mg, 29%. Anal. Calc. (found) (%): C, 24.22 (22.04); H, 6.50 (6.00); N, 10.11 (10.11). IR ($cm^{-1}$, KBr pellet): 3412 (vs), 3229 (s), 3165 (s), 2936 (m), 2878 (m), ≈1630 (w), 1473 (w), 1451 (w), 1429 (w), 1105 (m), 1071 (w), 1062 (w), 1016 (m), 1009 (m), 962 (s), 884 (m), 837 (s), 440 (w).

**Synthesis of $[Cu(C_{10}H_{24}N_4)][WO_4]\cdot 5.5H_2O$ (3)**

The transition metal source used was $NaWO_4\cdot 2H_2O$ (0.231 g, 0.7 mmol). The obtained crystals were purple. Yield: 32 mg, 26%. Anal. Calc. (found) (%): C, 20.57 (23.88); H, 5.52 (5.39); N, 9.60 (6.21). IR ($cm^{-1}$, KBr pellet): 3421 (vs), 3229 (s), 3165 (s), 2936 (m), 2878 (m), ≈1630 (w), 1473 (w), 1451 (w), 1429 (w), 1105 (m), 1071 (w), 1062 (w), 1016 (m), 1009 (m), 962 (s), 884 (m) 825 (s), 440 (w).

## 2.3. X-RAY CRYSTALLOGRAPHY

Crystal data for compounds **1**, **2** and **3** are given in Table 2. Data for compounds **2** and **3** were collected at 100 K on an Agilent Technologies Super-Nova diffractometer (graphite monochromated Mo Kα radiation, λ = 0.71073 Å, Sapphire CCD detector). In the case of compound **1**, data was collected at room temperature on an Agilent Technologies Super-Nova diffractometer (graphite monochromated Cu Kα radiation, λ = 1.54184 Å, Sapphire CCD detector). In the case of compound **3**, data frames were processed (unit cell determination, intensity data integration, correction for Lorentz and polarization effects, and analytical absorption correction) using the CrysAlis

software package. The three structures were solved using OLEX[47] and refined by full-matrix least-squares with SHELXL-97[48]. Final geometrical calculations were carried out with Mercury[49] and PLATON[50] as integrated in WinGX.

*Table 2.- Crystallographic Data for compounds **1**, **2** and **3**.*

| | **1** | **2** | **3** |
|---|---|---|---|
| **Formula** | $C_{10}H_{30}CrCuN_4O_7$ | $C_{10}H_{32}CuMoN_4O_8$ | $C_{10}H_{35}CuN_4O_{9.5}W$ |
| **MW (g mol$^{-1}$)** | 433.92 | 495.87 | 610.72 |
| **Crystal system** | Monoclinic | Monoclinic | Orthorhombic |
| **Space group** | $P2_1$ (4) | $P2_1/n$ (14) | Pbca (61) |
| **λ (Å)** | 1.54184 | 0.71073 | 0.71073 |
| **T (K)** | 273 | 100.0(1) | 100.0(1) |
| **a (Å)** | 10.4765(2) | 11.3931(2) | 14.2872(2) |
| **b (Å)** | 13.6774(2) | 14.5308(2) | 23.1050(3) |
| **c (Å)** | 12.5283(2) | 11.6281(2) | 12.3068(2) |
| **α (deg)** | 90.00 | 90.00 | 90.00 |
| **β (deg)** | 102.079(2) | 95.068(2) | 90.00 |
| **γ (deg)** | 90.00 | 90.00 | 90.00 |
| **V (Å$^3$)** | 1755.46(5) | 1917.51(6) | 4062.57(10) |
| **Z** | 4 | 4 | 8 |
| **Z'** | 2 | 1 | 1 |
| **$D_{calc}$ (g cm$^{-3}$)** | 1.642 | 1.718 | 1.961 |
| **μ (mm$^{-1}$)** | 6.952 | 1.805 | 6.754 |
| **Collected reflns** | 7501 | 14621 | 31087 |
| **Unique reflns ($R_{int}$)** | 2432 (0.027) | 3976 (0.030) | 4423 (0.049) |
| **Observed reflns [I > 2σ(I)]** | 2233 | 3583 | 3986 |
| **Parameters** | 433 | 329 | 229 |
| **R(F)[a] [I > 2σ(I)]** | 0.0263 | 0.0214 | 0.0412 |
| **wR(F$^2$)[a] (all data)** | 0.0756 | 0.0560 | 0.0835 |
| **GoF** | 1.057 | 1.081 | 1.269 |

[a]$R(F) = \sum||F_o| - |F_c||/\sum|F_o|$. $wR(F^2) = \{\sum[w(F_o^2 - F_c^2)^2]/\sum[w(F_o^2)^2]\}^{1/2}$.

# 3. RESULTS AND DISCUSSION

## 3.1. IR SPECTROSCOPY

As it can be seen in Figure 9, the IR spectra of compounds **1**, **2** and **3** only present differences in the region 950 – 800 $cm^{-1}$, which is characteristic of the oxyanion $[MO_4]^{2-}$ of the corresponding d-metal.[51,52] The remaining bands of the spectra are common in the three compounds, and are due to the Cu(*cyclam*) complex.[53,54]

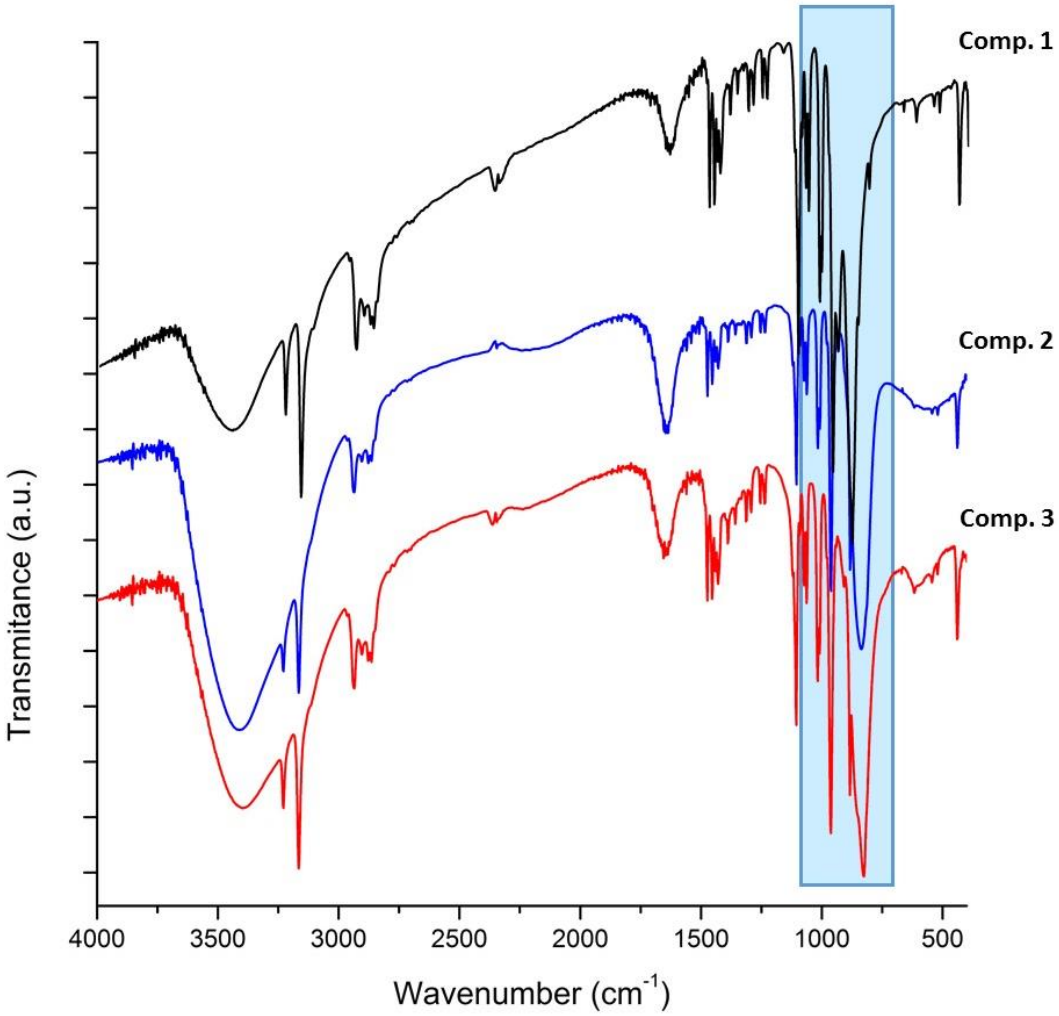


*Figure 9.- Infrared spectra of compounds **1**, **2** and **3** dispersed in KBr in the range from 4000 to 400 $cm^{-1}$. In blue it is marked the range where the oxyanions appear (950-800 $cm^{-1}$).*

In Figure 10, it can be seen that the first band of the IR spectrum, at 3421 $cm^{-1}$, is a wide band due to the hydrogen bond present between the water molecules, $\nu_{as}$ ($H_2O$). The two bands found at around 3229 and 3165 $cm^{-1}$ are due to the secondary amines found in *cyclam* molecule. The following bands at around 2936 $cm^{-1}$ and 2864 $cm^{-1}$ are assigned to $\nu_{as/s}$ $CH_2$ from Cu(*cyclam*) ligand.

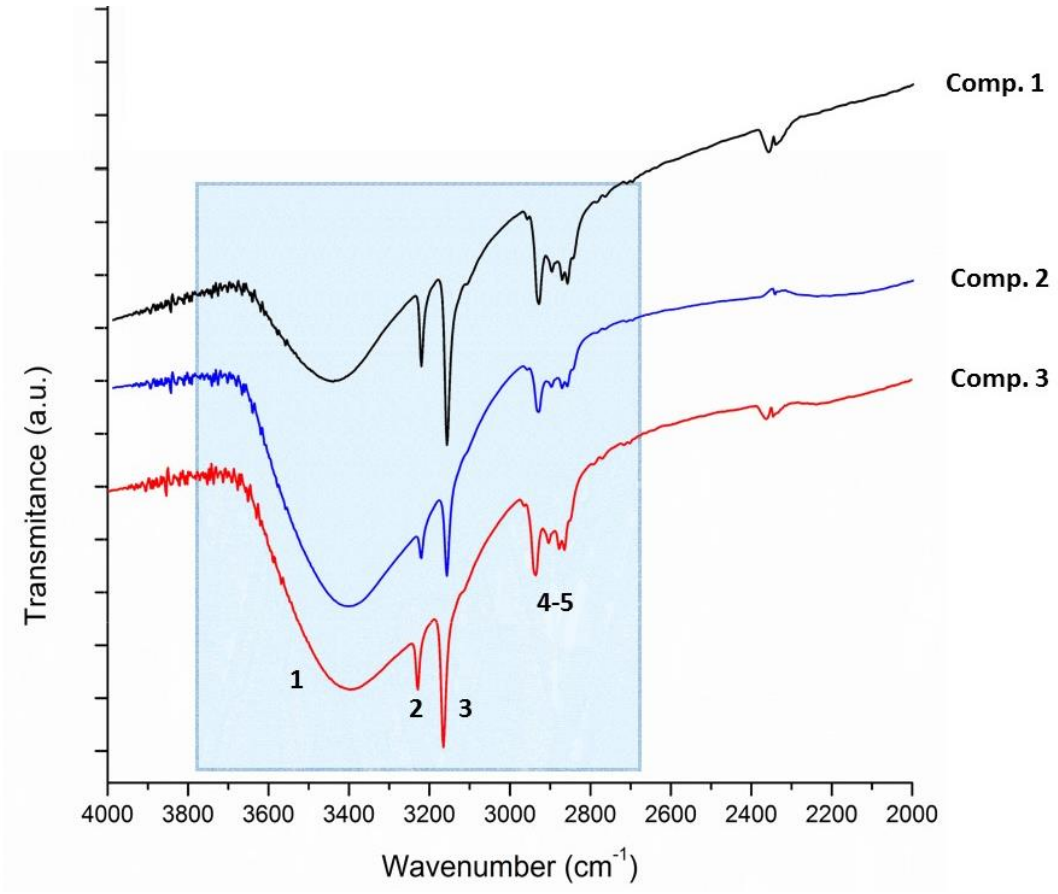


*Figure 10.- Infrared spectra of compounds **1**, **2** and **3** dispersed in KBr in the range from 4000 to 2000 $cm^{-1}$.*

All the bands found in the range between 1660 and 950 $cm^{-1}$ are characteristic from the Cu(*cyclam*) ligand, as shown in Figure 11. These band are assigned as δ NH, δ CH, δ CC and δ CN (Table 3).

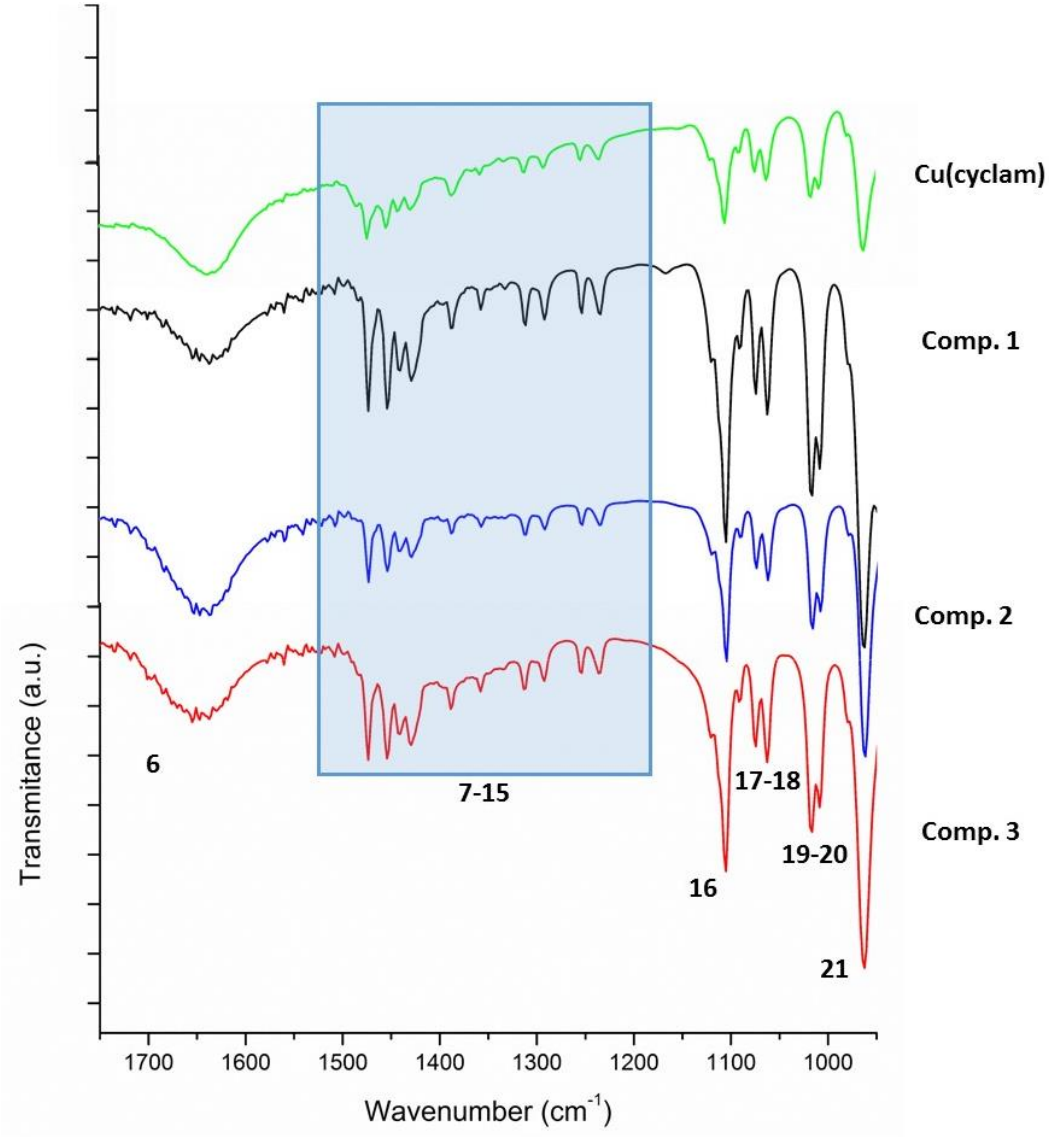


*Figure 11.- Infrared spectra of compounds **1**, **2** and **3** compared to that of Cu(cyclam) dispersed in KBr in the range from 1750 to 950 $cm^{-1}$.*

Then, another characteristic band from the Cu(*cyclam*) complex is the one found at 440 $cm^{-1}$ (Figure 12). This band is due to ν (Cu-N) mode, and it can be shown in the three compounds **1**, **2** and **3** as well as in the infrared spectrum of Cu(*cyclam*).

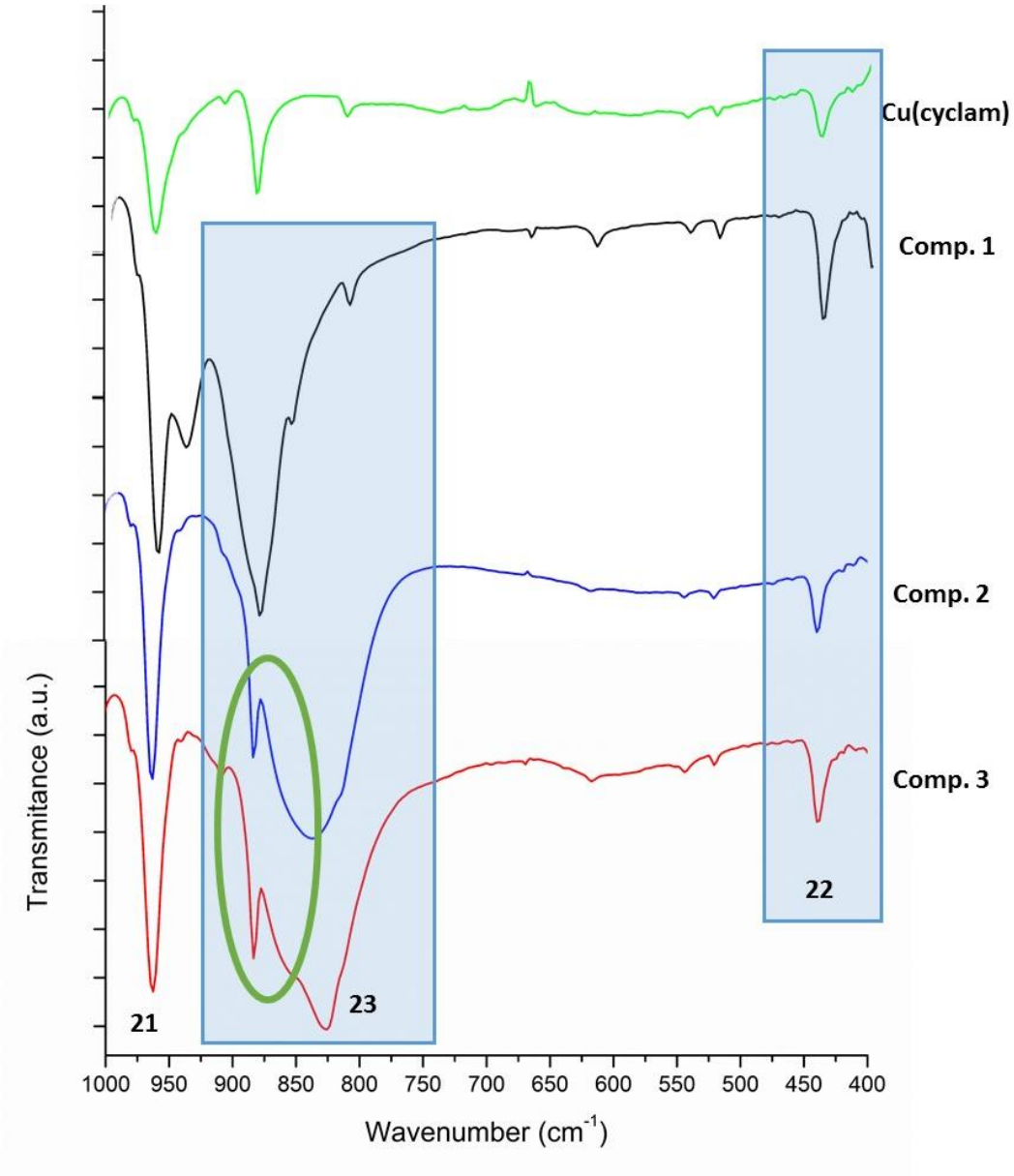


*Figure 12.- Infrared spectra of compounds **1**, **2** and **3** compared to that of Cu(cyclam) dispersed in KBr in the range from 1000 to 400 $cm^{-1}$. On the right the v (Cu-N) band is marked. On the left, the characteristic band of the oxyanions is marked.*

Finally, the characteristic bands of the tetrahedral oxyanions $[MO_4]^{2-}$ can be clearly identified in the range 950-800 $cm^{-1}$. The $[MO_4]^{2-}$ oxyanions can have 4 vibration modes shown in Figure 13.[51]

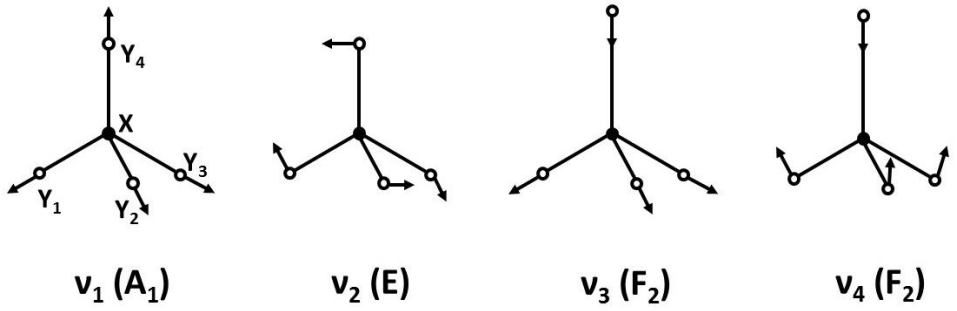


*Figure 13.- Normal modes of vibration of tetrahedral $[MO_4]^{2-}$ anion.*

The bands for the molybdate and tungstate appear at 837 and 825 $cm^{-1}$, respectively, while the characteristic band of chromate oxyanion appears a bit shifted to the left, at 883 $cm^{-1}$ (Figure 12 and Table 4). These three bands are due to vibration mode $\nu_3$ shown in Figure 13.

*Table 3.- Infrared frequencies characteristic from Cu(cyclam) found in compounds **1**, **2** and **3**.*

| Number | Vibration | Intensity | Signal ($cm^{-1}$) | | |
|---|---|---|---|---|---|
| | | | Comp. 1 | Comp. 2 | Comp. 3 |
| **1** | ν ($H_2O$) | Wide band | 3448 | 3412 | 3421 |
| **2** | ν (N-H) | Strong | 3229 | 3229 | 3229 |
| **3** | | Strong | 3165 | 3165 | 3165 |
| **4** | $\nu_{as/s}$ $CH_2$ | Medium | 2936 | 2936 | 2936 |
| **5** | | Weak | 2864 | 2878 | 2878 |
| **6** | δ NH<br>δ CH<br>δ CC<br>δ CN | Weak | ≈1630 | ≈1630 | ≈1630 |
| **7-15** | | Weak | 1500 – 1200 | | |
| **16** | | Medium | 1105 | 1105 | 1105 |
| **17** | | Weak | 1071 | 1071 | 1071 |
| **18** | | Weak | 1062 | 1062 | 1062 |
| **19** | | Weak | 1016 | 1016 | 1016 |
| **20** | | Medium | 1009 | 1009 | 1009 |
| **21** | | Strong | 962 | 962 | 962 |
| **22** | N (Cu-N) | Weak | 440 | 440 | 440 |

*Table 4.- Infrared frequencies characteristic from $[MO_4]^{2-}$ oxyanions in compounds **1**, **2** and **3**.*

| Signal number 23 | Vibration | Intensity | Signal ($cm^{-1}$) |
|---|---|---|---|
| **$[CrO_4]^{2-}$** | $v_3$ | Strong | 883 |
| **$[MoO_4]^{2-}$** | $v_3$ | Strong | 837 |
| **$[WO_4]^{2-}$** | $v_3$ | Strong | 825 |

Apart from the band shown in Table 4, there is another band, marked in green in the Figure 12, that appears in the spectra of compounds **2** and **3** at 884 $cm^{-1}$. It can be also seen that this band is due to the Cu(*cyclam*) ligand. In the IR spectrum of chromate this band cannot be seen as it is covered by the $v_3$ ($[CrO_4]^{2-}$) band.

### 3.2. CRYSTAL STRUCTURES FOR COMPOUNDS 1, 2 AND 3

Compounds **1** and **2** crystallize in the monoclinic space group $P2_1$ and $P2_1/n$, respectively, whereas compound **3** crystallizes in the orthorhombic space group Pbca. The asymmetrical unit of compound **1** contains two $[CrO_4]^{2-}$ anions, two $[Cu(cyclam)]^{2+}$ complexes and six water molecules. Whereas the asymmetrical unit of compound **2** and **3** contains only one $[MO_4]^{2-}$ anion and one $[Cu(cyclam)]^{2+}$ cataion. The water molecules are four for compound **2** and 5.5 disorder molecules over seven water positions for compound **3**. These asymmetric units, without the water molecules, are shown in Figure 14.

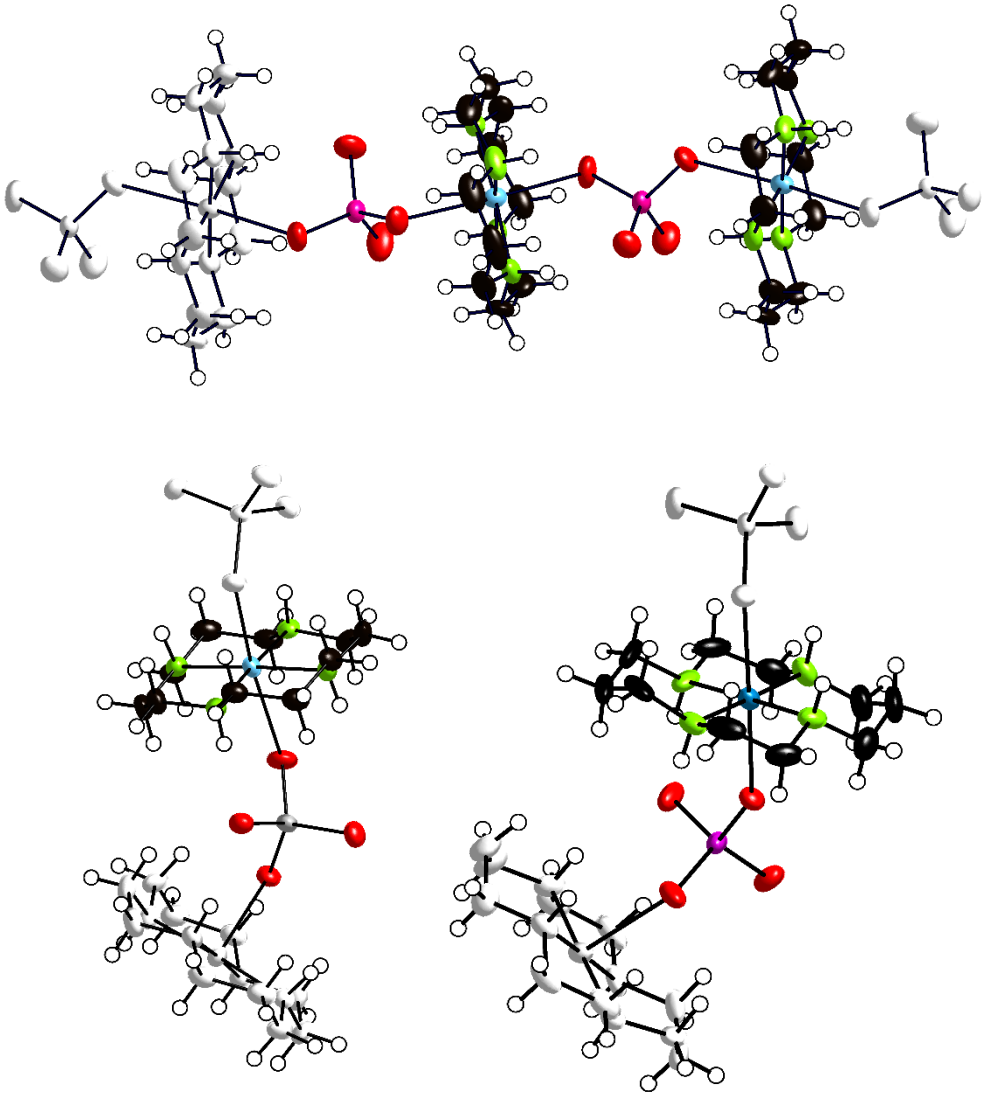

*Figure 14. ORTEP views of the asymmetric units (coloured) of compounds **1** (top), **2** (bottom left) and **3** (bottom right). Thermal ellipsoids: 1 (50%); 2 and 3 (70%).*

### 3.2.1. $[MO_4]^{2-}$ oxyanions

The $[MO_4]^{2-}$ oxyanions have a tetrahedral geometry which consists on an early transition metal (M = Cr, Mo, W) surrounded by four oxygen atoms which are directed toward the corners of the regular tetrahedron.

Table 5 displays selected bond lengths and angles for the $[MO_4]^{2-}$ oxyanions:

*Table 5.- Bond distances (Å) and angles (deg) for $[MO_4]^{2-}$ oxyanions.*

| Bond (Å) /Angle (deg) | $[CrO_4]^{2-}$ | | $[MoO_4]^{2-}$ | $[WO_4]^{2-}$ |
|---|---|---|---|---|
| | A | B | | |
| **M-O1** | 1.621(4) | 1.636(4) | 1.7513(15) | 1.755(4) |
| **M-O2** | 1.639(4) | 1.638(4) | 1.7714(15) | 1.792(5) |
| **M-O3** | 1.669(4) | 1.637(5) | 1.7792(14) | 1.772(5) |
| **M-O4** | 1.634(4) | 1.653(4) | 1.7599(15) | 1.783(5) |
| **O1-M-O4** | 110.9(2) | 109.5(2) | 110.35(7) | 110.4(2) |
| **O2-M-O3** | 107.1(3) | 110.3(3) | 109.23(7) | 108.7(3) |

Both M-O lengths and O-M-O are consistent with other $[MO_4]^{2-}$ clusters of group 6 metals (Cr, Mo and W) reported in the literature.[42,55,56]

Looking at the data for the bond distances M-Ox, it can be observed a tendency of the bonds to increase their length as the size of the early transition metal increases. As previously seen, chromium is smaller than molybdenum and tungsten, so that the M-Ox distances of the chromate oxyanion are the shortest ones, with a bond length average of 1.641 Å, while for molybdate and tungstate oxyanion M-Ox distances are longer, with an average of 1.7655 Å and 1.776 Å, respectively. M-Ox bond distances for molybdate and tungstate oxyanions are similar because Mo and W have similar size due to relativistic effects.

### 3.2.2. Cu(*cyclam*) complexes

The three oxyanions of compounds **1**, **2** and **3** are bonded to the $[Cu(cyclam)]^{2+}$ organic ligand. As shown in the asymmetric units (Figure 14), the coordination spheres of the copper centres show distorted octahedral $CuN_4O_2$ geometries with the four N atoms of the *cyclam* ligand forming the equatorial plane and the axial position occupied by terminal O atoms from the oxyanions. All the complex found in the structure of compound **1**, **2** and **3** present the so-called *trans-III* configuration (Figure 7), that is, two N-H bonds above and the other two below the $CuN_4$ equatorial plane.

In Table 6 the $Cu_1$-Nx and $Cu_1$-Ox bond distances of Cu(cyclam) and oxyanions in the three compounds are shown, as well as Cu···Cu distances and CShM ($O_h$) distortion and O1-Cu-O4, Cu1-M-Cu1 and Cu(*cyclam*)^Cu(*cyclam*) angles.

*Table 6.- Bond distances and angles for Cu(cyclam) complexes.*

| | **1** | | **2** | **3** |
|---|---|---|---|---|
| | **A** | **B** | | |
| **Bond distances (Å)** | | | | |
| **Cu-N1** | 2.017(4) | 2.030(5) | 2.0177(2) | 2.032(6) |
| **Cu-N4** | 2.005(4) | 2.024(5) | 2.0267(2) | 2.009(6) |
| **Cu-N8** | 2.011(4) | 2.006(5) | 2.0117(2) | 2.027(6) |
| **Cu-N11** | 2.024(5) | 2.003(4) | 2.0214(2) | 2.002(6) |
| **Cu-O1** | 2.389(4) | 2.397(4) | 2.3217(1) | 2.398(4) |
| **Cu-O4** | 2.538(4) | 2.519(4) | 2.7454(2) | 2.564(4) |
| **Cu···Cu** | 7.302(7) | 7.252(7) | 7.2902(4) | 7.1852(10) |
| **Angles (deg)** | | | | |
| **O1-Cu-O4** | 174.9(2) | 173.0(2) | 173.07(7) | 173.7(2) |
| **Cu1-M-Cu1** | 166.1(2) | 167.3(2) | 139.93(8) | 131.2(2) |
| **Cu(*cyclam*)^Cu(*cyclam*)** | 47.4 | 47.4 | 31.2 | 44.4 |

The lengths and angles found for Cu(*cyclam*) are consistent with the ones reported in the literature.[57]

The Cu···Cu distances decreases when going down in the group 6 of the periodic table. This is because the angle Cu-M-Cu also decreases in the same direction and, therefore, the smaller angle, the shorter Cu-Cu distance.

*Table 7.- Parameters for calculating the distortion of the Cu coordination polyhedral, being Δ the difference between axial and equatorial bond distances, TPR the ideal trigonal prism and CShM($O_h$) Continuous Shape Measurement of the octahedral geometry.*

| | 1 | | 2 | 3 |
|---|---|---|---|---|
| | A | B | | |
| **Equatorial bond average (Å)** | 2.014 | 2.016 | 2.0194 | 2.017 |
| **Axial bond average (Å)** | 2.463 | 2.458 | 2.5586 | 2.481 |
| **Δ** | 0.449 | 0.442 | 0.5392 | 0.464 |
| **CShM ($O_h$)** | 1.132 | 1.120 | 1.613 | 1.224 |
| **TPR** | 16.362 | 15.734 | 16.276 | 16.395 |
| **EQ. 5** | 0.938 | 0.907 | 1.389 | 1.007 |
| **EQ. 6** | -0.395 | -1.167 | -0.500 | -0.354 |
| **EQ. 7** | 5.109 | 5.025 | 5.304 | 5.155 |
| **EQ. 8** | 1.618 | 1.579 | 2.177 | 1.705 |
| **EQ. 9** | 3.238 | 3.201 | 3.769 | 3.320 |

$$Csh(O_h) = 5.39 \cdot \Delta^2 - 0.33 \cdot |\Delta| \qquad (\boldsymbol{Eq.5})$$

$$Csh(O_h) = 1.23 \cdot TPR - 20.52 \qquad (\boldsymbol{Eq.6})$$

$$\sqrt{CShM(O_h)} + \sqrt{TPR} = 4.16 \qquad (\boldsymbol{Eq.7})$$

$$\theta = 50^o : Csh(O_h) = 0.53 + 6.258 \cdot \Delta^2 - 0.172 \qquad (\boldsymbol{Eq.8})$$

$$\theta = 40^o : Csh(O_h) = 2.08 + 6.118 \cdot \Delta^2 - 0.167 \cdot \Delta \qquad (\boldsymbol{Eq.9})$$

The metal centres in the Cu(*cyclam*) complex presents a distorted octahedral geometry (Table 7). The degree of such distortion has been analysed by Continuous

Shape Measurement analyses using SHAPE software. If equations 5 and 6 were obey, the Cu(*cyclam*) complex would have an ideal Jahn-Teller distortion. On the contrary, if equation 7 was obey, the ligand would have an ideal Bailar distortion.

As it can be seen in Table 7, none of the compounds fulfil the equations. Thus, the Cu(*cyclam*) for the three compounds **1**, **2** and **3** present a combined effect of Jahn-Teller and Bailar distortions of the octahedron.

A compound with this distortion can have a twist angle of 40°, 50° or 60°, being 60° an ideal Jahn-Teller distortion. As equation 6 is not fulfilled, the Cu(*cyclam*) ligand does not present an angle twist of 50°. However, the equation 9 fits less with the CShM($O_h$). Thus, the Cu(*cyclam*) ligand has an angle between 50°-60°.

To sum up, the Cu(*cyclam*) of the three compounds **1**, **2** and **3** present a combined effect of Jahn-Teller and Bailar distortion of the octahedron symmetry, with a twist angle between 50°-60°.

The Jahn-Teller distortion consist on an elongation of the axial bonds and a contraction of the equatorial ones, leading from a $O_h$ symmetry to a $D_{4h}$ one. The Bailar distortion consist on twist the angle of the equatorial bonds by leading to a $D_{3h}$ symmetry (Figure 15).[58,59]

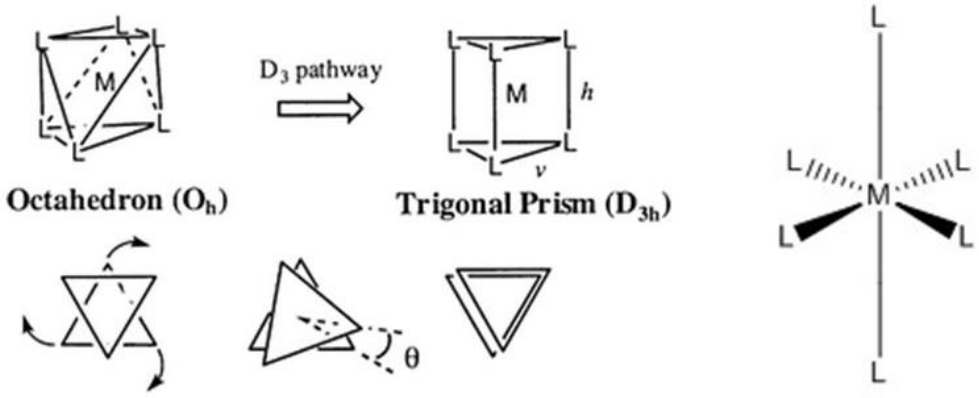


*Figure 15.- Schematic description of Bailar twist (on the left) and Jahn-Teller distortion (on the right).*

### 3.3. CRYSTAL PACKING FOR COMPOUNDS 1, 2 AND 3

The three compounds present a 1-D character because they are formed by parallel chains of $\{[Cu(cyclam)][MO_4]\}_\infty$. In the chains, Cu(*cyclam*) complexes are connected through two separate oxygens from the $[MO_4]^{2-}$ group, which occupy the axial coordination positions of copper(II) atoms, as previously seen in the asymmetric units (Figure 14).

#### 3.3.1. Crystal Packing of $[Cu(C_{10}H_{24}N_4)][CrO_4]\cdot 3H_2O$ (1)

Compound **1** is made up of antiparallel chains running along the [101] direction (Figure 16). This chains contain the repeated unit $\{[Cu^{1A}][Cr^{1A}][Cu^{1B}][Cr^{1B}]\}$ formed by an alternative sequence of cation complexes and anions. As it can be also seen that the chains are bonded together by $C\text{-}H_{Cu(cyclam)}\cdots O_{OA}$ hydrogen bonds, forming corrugated layers which are parallel to (10-1) plane.

In Figure 17, it can be seen that no water molecules are located between the chains, but they are located between the corrugated layer. Thus, the water molecules contribute to the linking between the layers by forming an extensive hydrogen bond network (Table 8).

Apart from the intermolecular hydrogen bonds, there are also intramolecular hydrogen bonds (Table 8), which help to the packing of the $[Cu(cyclam)[MO_4]$ units.

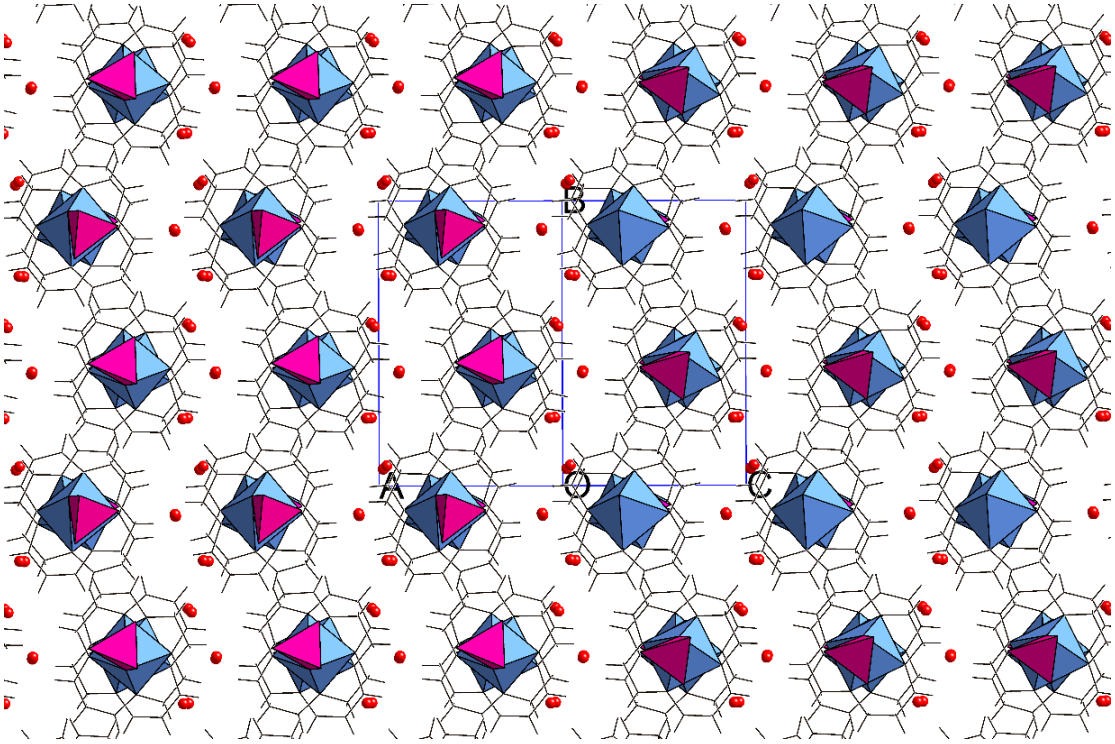


*Figure 16.- View of the crystal structure of compound **1** along the direction [101].*

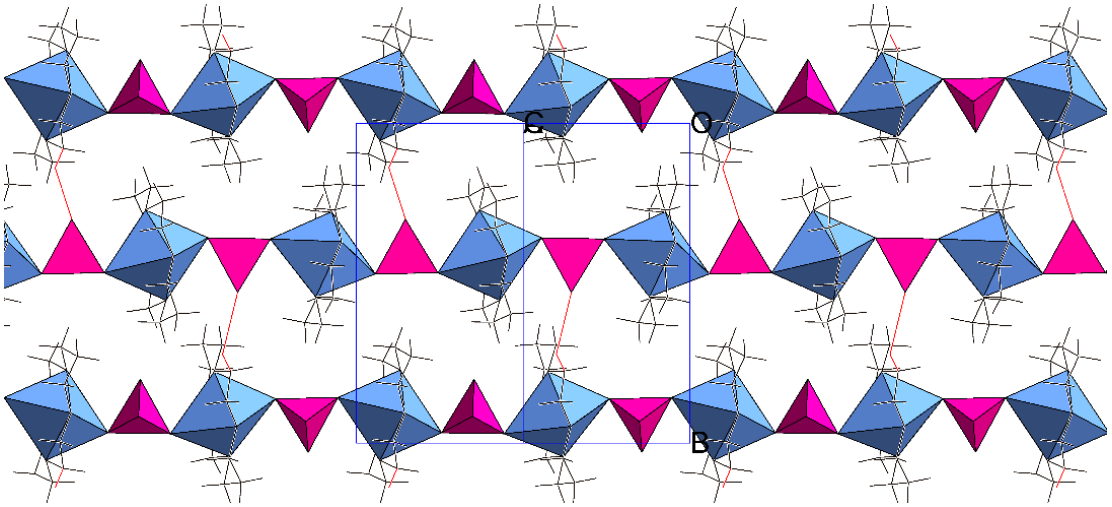


*Figure 17.- View of the chains of compound **1** in the plane perpendicular to (10-1).*

*Table 8. Intermolecular and intramolecular contacts for compounds **1**.*

| Intermolecular hydrogen bonds | | | |
|---|---|---|---|
| **D-H···A** | **D-H** | **D···A (Å)** | **Angle (deg)** |
| **N1A-H1A···O6A** | 0.91 | 3.242(6) | 134 |
| **O7A-H7AC···O6A** | 0.85 | 2.827(8) | 145 |
| **O7A-H7AC···O4A** | 0.85 | 3.011(7) | 167 |
| **O6B-H6BC···O3B** [i] | 0.85 | 2.778(8) | 157 |
| **O6B-H6BD···O5B** | 0.85 | 2.780(8) | 171 |
| **O5B-H5BC···O2A** [ii] | 0.85 | 2.759(7) | 150 |
| **O5B-H5BD···O6B** | 0.85 | 2.780(8) | 107 |
| **O6A-H6AD···O2B** [iii] | 0.85 | 2.775(6) | 145 |
| **C7B-H7BC···O4B** [iv] | 0.85 | 3.000(6) | 170 |
| **O7B-H7BD···O7A** | 0.85 | 2.923(8) | 150 |
| **O5A-H5AC···O6B** | 0.85 | 2.783(8) | 149 |
| **O5A-H5AD···O3A** | 0.85 | 2.769(7) | 158 |
| **C10A-H10D···O3B** [v] | 0.97 | 3.200(7) | 140 |
| **C2A-H2AA···O6B** [iv] | 0.97 | 3.399(9) | 141 |
| **C9B-H9BA···O3A** | 0.97 | 3.434(7) | 130 |
| **Intramolecular hydrogen bonds** | | | |
| **N1B-H1B···O3A** | 0.91 | 3.359(6) | 162 |
| **N4A-H4A···O3B** | 0.91 | 3.221(5) | 167 |
| **N8A-H8A···O2A** | 0.91 | 2.959(5) | 169 |
| **N8B-H8B···O3B** [vi] | 0.91 | 3.199(6) | 154 |
| **N11A-H11A···O3A** | 0.91 | 3.088(6) | 157 |
| **N11B-H11B···O2A** | 0.91 | 2.985(6) | 171 |
| **C12A-H12D···O4B** | 0.97 | 3.180(7) | 123 |

*Symmetry codes (i) 1-x,1/2+y,1-z. (ii) 1-x, 1/2+y, -z. (iii) -1+x, y, z. (iv) 1-x, -1/2+y, 1-z. (v) 2-x, 1/2+y, 1-z. (vi) -1+x, y, -1+z.*

*Table 9. Distances between Cr and Cu of adjacent chains.*

| D···A | Distance (Å) |
|---|---|
| **Cr1A-Cu1B** | 7.276 |
| **Cr1A-Cu1B** | 7.069 |
| **Cr1A-Cr1B** | 13.677 |
| **Cu1A···Cu1B** | 13.677 |

The distances between the chains (Table 9) make suitable the presence of the hydrogen bonds of Table 8.

### 3.3.2. Crystal Packing of $[Cu(C_{10}H_{24}N_4)][MoO_4]\cdot 4H_2O$ (2)

The crystal packing of compound **2** along the [010] direction is displayed in Figure 18. As the chains are further away each other than in compound **1** (Table 9 vs. 11), there are not direct hydrogen bonding interactions between Cu(*cyclam*) and the oxyanion (Figure 19). In this compound the chains are held together by hydrogen interactions that involves to water molecules of type C-$H_{Cu(cyclam)}\cdots O_w\cdots O_{OA}$ (Table 10).

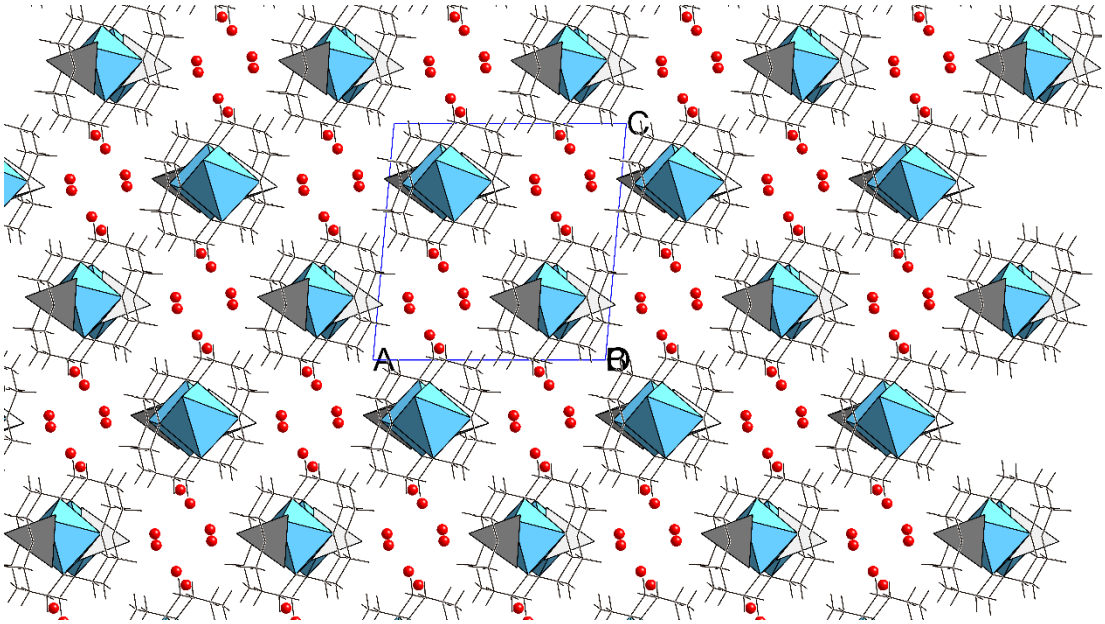


*Figure 18.- View of the crystal structure of compound **2** along the direction [010].*

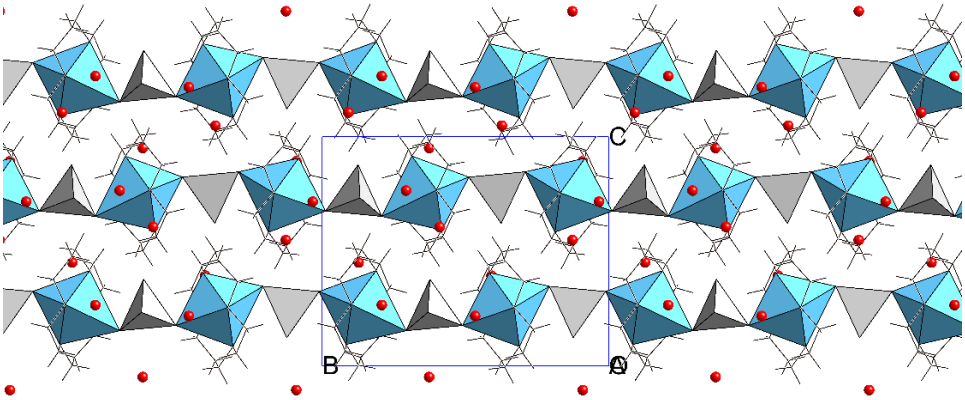


*Figure 19. View of the chains located in the plane (01-1).*

*Table 10.- Intermolecular and intramolecular contact for compounds **2**.*

| **Intermolecular hydrogen bonds** | | | |
|---|---|---|---|
| **D-H···A** | **D-H** | **D···A (Å)** | **Angle (deg)** |
| **N1-H1···O5** | 0.91 | 3.0485 | 139 |
| **O5-H5C···O2** [i] | 0.84 | 2.6611 | 167 |
| **O6-H6C···O2** [ii] | 0.79 | 2.7395 | 168 |
| **O6-H6D···O8** | 0.80 | 2.7604 | 166 |
| **O7-H7C···O4** | 0.81 | 2.8850 | 175 |
| **O7-H7D···O6** | 0.77 | 2.7860 | 164 |
| **N8-H8···O6** [iii] | 0.91 | 2.9513 | 159 |
| **O8-H8A···O5** [iv] | 0.81 | 2.7201 | 156 |
| **O8-H8B···O3** [v] | 0.81 | 2.7430 | 168 |
| **Intramolecular hydrogen bonds** | | | |
| **N4-H4···O3** | 0.91 | 3.0785 | 168 |
| **N11-H11···O3** [i] | 0.91 | 2.9645 | 172 |

*Symmetry codes (i) 1/2-x, -1/2+y, 1/2-z. (ii) 1/2+x, 1/2-y, 1/2+z. (iii) -1/2+x, 1/2-y, -1/2+z. (iv) -1/2+x, 1/2-y, 1/2+z. (v) 1/2-x, -1/2+y, 3/2-z.*

*Table 11.- Distances between Mo and Cu of different antiparallel chains.*

| **D···A** | **Distance (Å)** |
|---|---|
| **Mo···Cu** | 6.586 |
| **Mo···Cu** | 9.101 |
| **Mo···Mo** | 15.544 |
| **Cu···Cu** | 15.544 |

In compound **2**, the water molecules are located in the space between the chains, as seen in Figure 20. The arrangement of water molecules generates hydrophilic regions formed by two waterfalls at x=0.25; z=0.75 and x=0.75; z=0.25. The waterfalls are formed by squares hydrogen bonded water molecules running parallel to y axis.

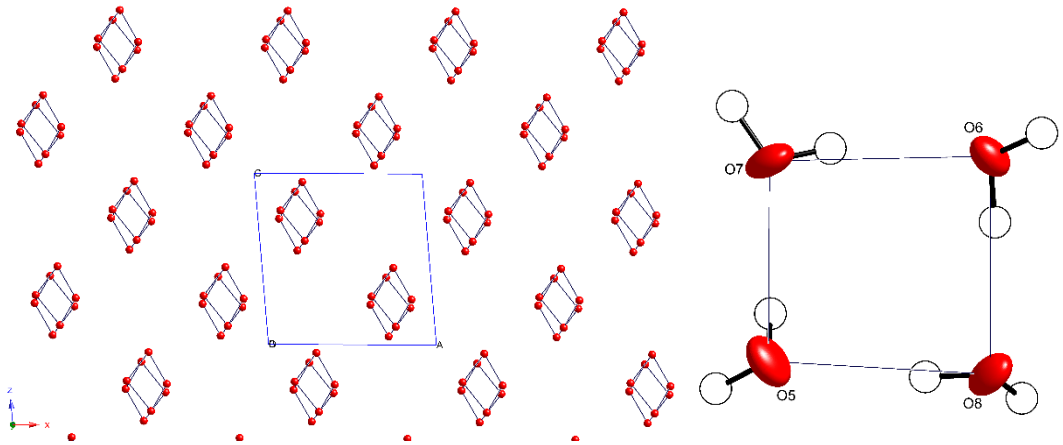


*Figure 20.- The arrangement of water molecules in compound **2** along the direction [010].*

### 3.3.3. Crystal Packing of $[Cu(C_{10}H_{24}N_4)][WO_4]\cdot 5.5H_2O$ (3)

Figure 21 shows the view of crystal structure of compound **3** along in the plane (100).

The compound **3** consists of corrugated layer formed by single chains that are hydrogen bonded between them through O9 water molecule (Figure 22) (Table 12).

The corrugated layers are packed along the [010] direction generating cavities between layers where the rest of water molecules are located.

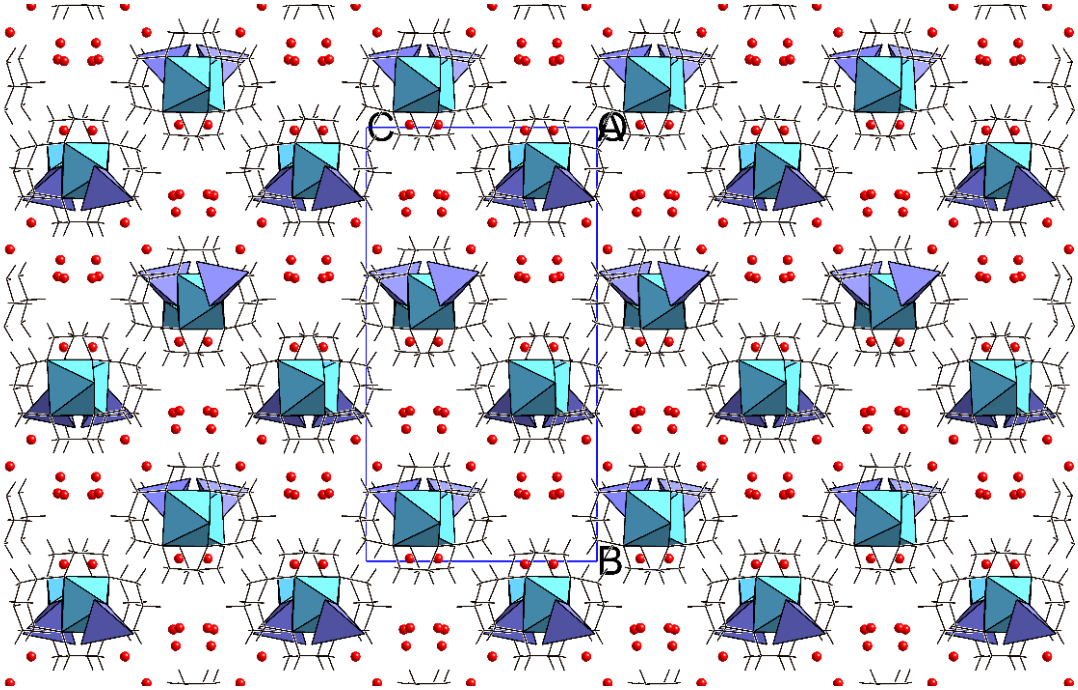


*Figure 21.- View of crystal structure of compound **3** along the [100]direction.*

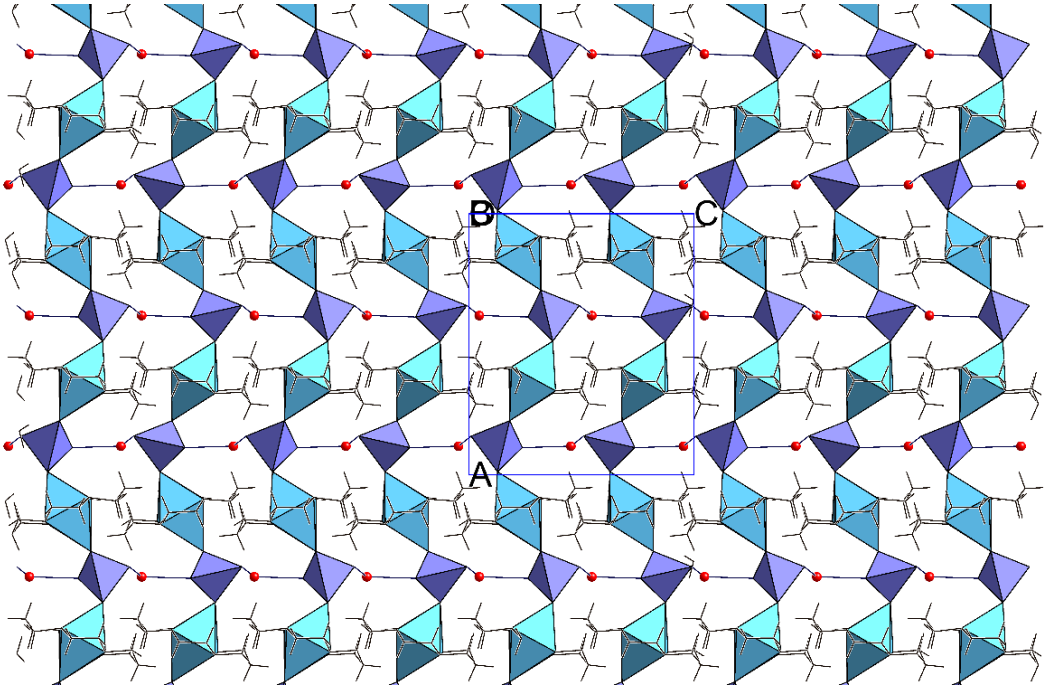


*Figure 22.- View of the chains of compound **3** in the plane (101).*

*Table 12.- Intermolecular and intramolecular contacts for compounds **3**.*

| Intermolecular hydrogen bonds | | | |
|---|---|---|---|
| **D-H···A** | **D-H** | **D···A (Å)** | **Angle (deg)** |
| **N8-H8···O11** | 0.91 | 3.107(8) | 171 |
| **N11-H11···O11** [i] | 0.91 | 3.018(8) | 160 |
| **C3-H3A···O8** | 0.97 | 3.466(9) | 149 |
| **C5-H5A···O7** [ii] | 0.97 | 3.412(1) | 150 |
| **C6-H6A···O5** [iii] | 0.97 | 3.211(1) | 134 |
| **C13-H13B···O5** | 0.97 | 3.444(1) | 152 |
| **C13-H13B···O6** | 0.97 | 3.512(1) | 160 |
| **Intramolecular hydrogen bonds** | | | |
| **N1-H1···O3** | 0.91 | 3.072(8) | 165 |
| **N4-H4···O3** [iv] | 0.91 | 3.445(8) | 157 |

*Symmetry codes (i) -1/2+x, y, 1/2-z. (ii) -1/2+x, 1/2-y, -z. (iii) x, y, -1+z. (iv) 1/2+x, y, 1/2-z.*

*Table 13.- Distances between W and Cu of different chains.*

| **D···A** | **Distance (Å)** |
|---|---|
| **W-Cu** | 6.981 |
| **W-Cu** | 9.616 |
| **W-W** | 8.101 |
| **Cu-Cu** | 9.296 |

### 3.4. ELECTRON PARAMAGNETIC RESONANCE (EPR)

The EPR Q-bands for compounds **2** and **3** (Figures 23 and 24) are characteristic of an octahedral coordinated $Cu^{2+}$. The Q-bands show that compounds **2** and **3** belong to the rhombic system, with an elongated octahedral or squared based pyramidal geometry (Table 14). $Cu^{2+}$ has a spin S = ½ with a nuclear spin of I = 3/2 and, as it is not magnetically isolated, there is no presence of four-line hyperfine splitting.

*Table 14.- The values of "g" from the Band-Q of the EPR spectra.*

| | **Comp. 2** | **Comp. 3** |
|---|---|---|
| **$g_1$** | 2.051 | 2.051 |
| **$g_2$** | 2.073 | 2.073 |
| **$g_3$** | 2.177 | 2.179 |

If G values are calculated by Equation 10, a value of 2.85 is obtained for compound **2** and 2.89 for compound **3**. For the obtaining G values, it has been assumed that the $g_z$ was the g with the highest value.

$$G = \frac{g_z - 2}{\frac{g_x + g_y}{2} - 2} \qquad (\boldsymbol{Eq.\ 10})$$

Having a G value lower than 4 indicates that the $Cu^{2+}$ of both compounds do not have the same orientation along the chains, what has been observed in the crystal packing for compounds **2** and **3**.

There Cu(*cyclam*)^Cu(*cyclam*) angles previously seen in Table 6, show a higher misalignment between the principal axes than the G values. This may be due to the fact that we have considered the crystal planes to be the same as the magnetic planes.

In addition, if we compared the two Q-band of compounds **2** and **3**, it can be seen that there is a higher difference between the $g_1$ and $g_3$ values for compound **3** than for compound **2** (Figure 25). This little difference is also matches with the G values, as the value for compound **3** is a bit higher than the one for compound **2**.

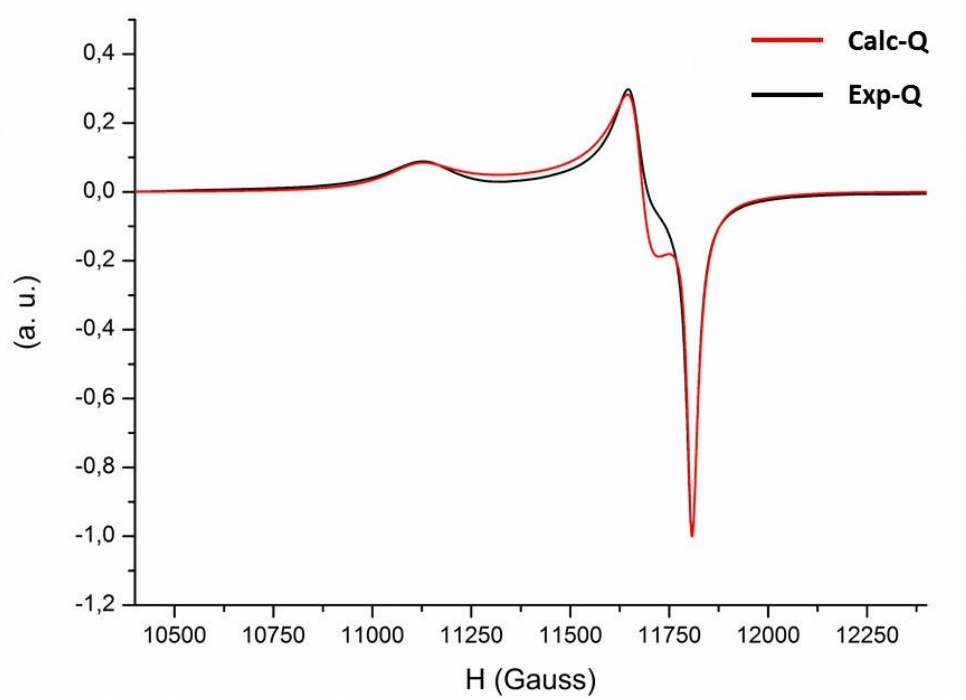


*Figure 23.- Q-band for compound **2**.*

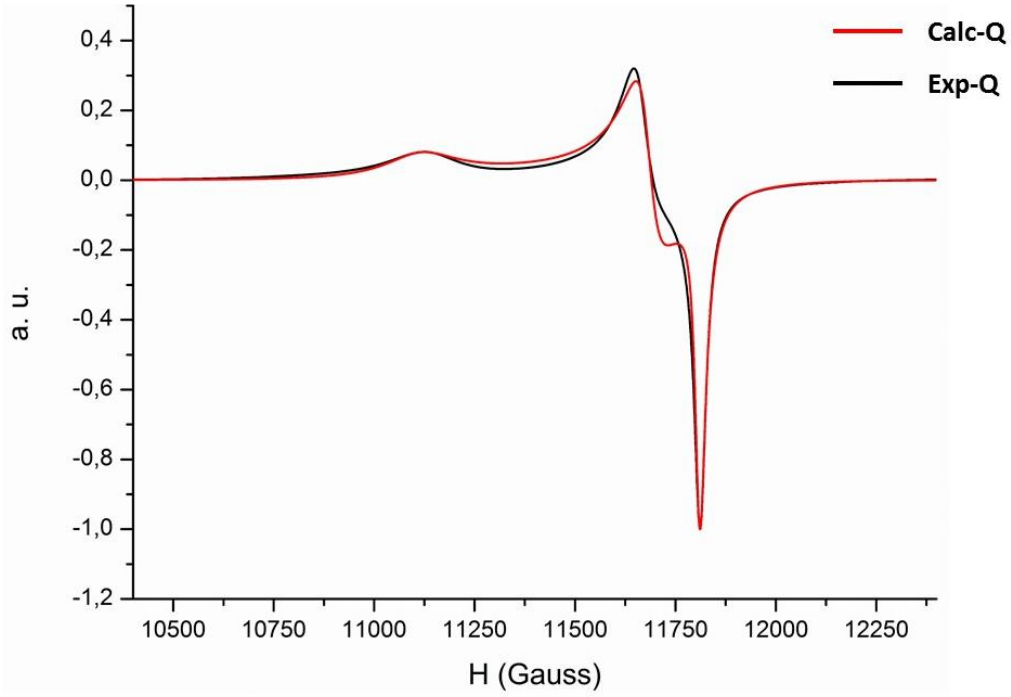


*Figure 24.- Q-band for compound **3**.*

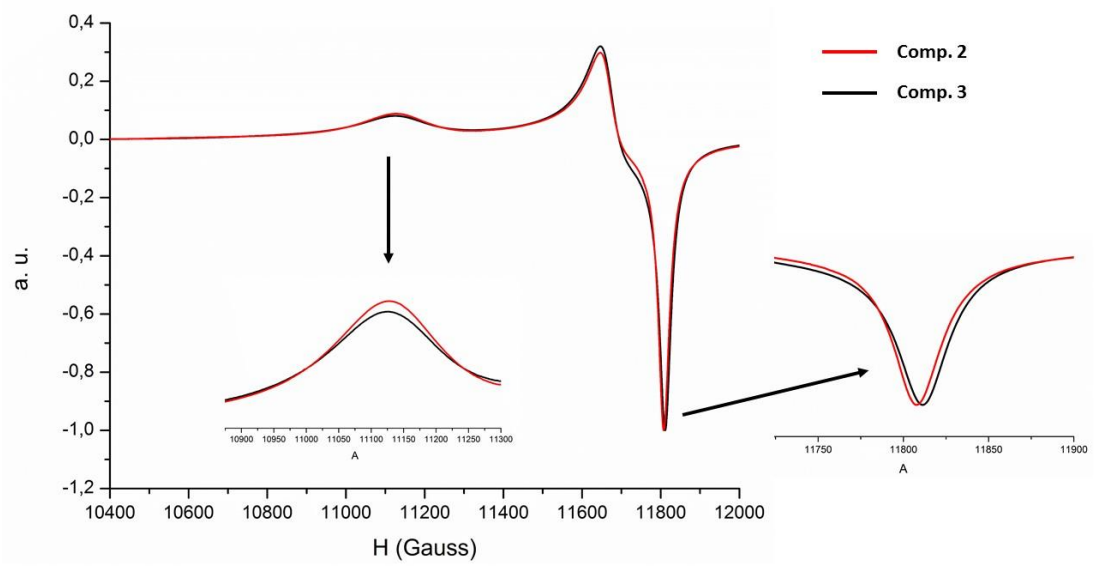


*Figure 25.- Comparing the Q-bands for compound **2** and **3**.*

## 4. CONCLUSIONS

Three new compounds have been prepared based on group 6 transition metal oxyanions with the metal-organic ligand Cu(*cyclam*). The three compounds have been characterized by IR spectroscopy and their structure described by X-ray diffraction.

The three compounds show a similar packing but with significant differences. All crystal packings consist of endless chains formed by the repetition of the $\{[Cu(cyclam)]MO_4\}_\infty$. The chains are parallel or antiparallel between them, and with a different degree of hydration.

The angles and interaction between the chains differ in the three compounds, which affect to their 3D packaging. These remarkable differences also affect to the magnetic properties, as observed in the EPR studies.

## 5. FUTURE WORK

Improve the synthetic methods in order to obtain the compounds pure with a higher degree of purity. It would be of great interest to do a study of the magnetic properties of the three compounds, as well as an EPR study in depth. A thermo-diffractogram and the study of the crystal structures of the anhydrous species would be also interesting as the thermogravimetric studies of compounds **1**, **2** and **3**, when they have been dehydrated, reveal a stable region between 100-250 °C, similar to that shown in different Cu(*cyclam*) polyoxometalate compounds in which the crystal structure of both the hydrated and anhydrous species have been measured.

Thermogravimetric studies also allow us to observe and study the possible single-crystal-to-single-crystal phase transition promoted by dehydration processes.

Finally, the study of the oxyanions could be extended to $[SO_4]^{2-}$ and $[SeO_4]^{2-}$ anions as $[MO_4]^{2-}$ representatives.

## 6. ACKNOWLEDGEMENTS

This project has been carried out at *Departamento de Química Inorgánica de la Facultad de Ciencia y Tecnología de la Universidad del País Vasco UPV/EHU*, under the direction of Dr. Juan Manuel Gurierrez-Zorrilla and Dr. Beñat Artetxe. I would like to thank both for their help and support in this project and for the opportunity they give me to do the end-of-degree project in their research team.

I would also like to thank all the technicians from SGIker (UPV/EHU) responsible of the analysis included in this research. Dra. Leire San Felices, Dr. Luis Lezama, Jagoba Martín and Dr. Luis Bartolomé also should be acknowledged for single crystal X-ray diffraction, EPR, TG and CHN experiments, respectively.

## 7. REFERENCES

(1) Ammam, M. *J. Mater. Chem. A*, **2013**, *1*, 6291.

(2) Miras, H. N.; Yan, J.; Long, D. L.; Cronin, L. *Chem. Soc. Rev.* **2012**, *41*, 4703-7430.

(3) Pope, M. T. *Heteropoly and Isopoly Oxometalates*; Springer-Verlag: Berlin, **1983**.

(4) Reinoso, S. Complejos Dinucleares Cobre(II)-Carboxilato Puente Soportados sobre Polioxometalatos Tipo Keggin. Ph.D. Universidad del País Vasco, UPV/EHU, Leioa, Spain, 2005.

(5) Sha, J.; Peng, J.; Lan, Y.; Su, Z.; Pang, H.; Tian, A.; Zhang, P.; Zhu, M. *Inorg. Chem.* **2008**, *47*, 5145-5153.

(6) Klemperer, W. G. *Inorg. Synth.* **1990**, *27*, 71.

(7) Crans, D. C.; Tracey, A. S. The Chemistry of Vanadium in Aqueous and Nonaqueous Solution. In *Vanadium Compounds: Chemistry, Biochemistry, and Therapeutic Applications*; American Chemical Society: Washington, DC, 1998; pp 2-29.

(8) Pyrzynska, K. *Chem. Anal. (Warsaw)* **2006**, *51*, 339.

(9) Etxebarria, N. Some Hydrolitic Equilibria of Mo(VI), V(VI), Nb(V) and Ta(V). Ph.D. Universidad del País Vasco, UPV/EHU, Leioa, Spain, 1993.

(10) Haight, G. P.; Boston, D. R. *J. Less-Common Met.* **1974**, *36*, 95-102.

(11) Ho, P. H.; Stroobants, K.; Parac-Vogt, T. N. *Inorg. Chem.* **2011**, *50*, 12025-12033.

(12) Di Natale, F.; Lancia, A. *Ind. Eng. Chem. Res.* **2007**, *46*, 6777-6782.

(13) Greenwood, N. N.; Earnshaw, A. Chromium, Molybdenum and Tungsten. In *Chemistry of the Elements;* Butterworth Heinemann: University of Leeds, U.K., 1997; pp 1002-1039.

(14) Bailey, N.; Carrington, A.; Lott, K. A. K.; Symons, M. C. R. *Chem. Rev.* **1963**, *63* (5), 443-460.

(15) Wulfsberg, G. Metal Cations and Oxo Anions in Aqueous Solution. In *Principles of Descriptive Inorganic Chemistry*; Brooks/Cole: Monterey, California, 1987; pp 21-58.

(16) Averill, B. A.; Eldredge, P. The d-Block Elements. In *Principles of General Chemistry* (v. 1.0M) http://bit.ly/1R6V7kp Free Online Book

(17) Wulfsberg, G. The Underlying Reasons for Periodic Trends. In *Principles of Descriptive Inorganic Chemistry*; Brooks/Cole: Monterey, California, 1987; pp 371-401.

(18) Pyykkö, P. *Chem. Rev.* **1998**, *88*, 563-594.

(19) Krebs, R. E. Transition Elements: Metals to non-metals. In *The History and Use of Our Earth's Chemical Elements: A Reference Guide*; Greenwood: Westport, Connecticut, London, 1922; pp 85-172.

(20) Dellien, I.; Hall, F. M.; Hepler, L. G. *Chem. Rev.* **1976**, *76* (3), 283-310.

(21) De Luyart, F.; De Luyart, J. J. *Análisis Química del Volfram, y Examen de un Nuevo Metal, que Entra en su Composición; Extractos de las Juntas Generales celebradas por la Real Sociedad Bascongada de Amigos del País:* Vitoria, Spain, 1783; pp 46-88.

(22) Kallmann, S. *Anal. Chem.* **1955**, *27* (9), 1433-1435.

(23) Rooley, J.; Rohrer, C. S.; Brown, O. W. *J. Phys. Chem.* **1952**, *56* (9), 1082-1084.

(24) Ripperger, W.; Saum, W. *J. Less-Common Met.* **1977**, *54*, 353-362.

(25) Grasselli, R. K. Molybdate and Tungstate Catalysts for Methanol Oxidation. In *Solid-State Chemistry in Catalysis;* American Chemical Society, Washington, DC, 1985; pp 103-119.

(26) Eastaugh, N.; Walsh, V.; Chaplin, T.; Siddall, R. Pigment Classification. In *Pigment Compendium: A Dictionary and Optical Microscopy of Historical Pigments*; Routledge: New York, NY, 2008; pp 417-463.

(27) Simpson, C. The Replacement of Chromate- and Lead-Based Inhibitors in Prospective Coatings. In *Organic Coatings for Corrosion Control;* Bierwagen G. P., Ed.; American Chemical Society: Washington, DC, 1998; pp 356-365.

(28) Dariva, C. G.; Galio, A. F. Corrosion Inhibitors – Principles, Mechanisms and Applications. In *Developments in Corrosion Protection;* Aliofkhazraei, M, Ed.; InTech: Winchester, U.K., 2014.

(29) Shkirskiy, V.; Keil P.; Hintze-Bruening H.; Leroux F.; Vialat P.; Lefèvre G.; Ogle K.; Volovitch P. *Appl. Mater. Interfaces*, **2015**, *7* (45), 25180-25192.

(30) Casas, J. S.; Moreno, V.; Sánchez, A.; Sánchez, J. L.; Sordo, J. Bioquímica del Molibdeno y del Wolframio: Oxotransferasas y nitrogenasas. In *Química Bioinorgánica;* Síntesis: Madrid, Spain, 2002; pp 163-190.

(31) Christian, J.; Singh Gaur, R. P.; Wolfe, T.; Trasorras, J. R. L. Tungsten Chemicals and their Applications. *Global Tungsten and Powders Corp.,* Towanda, PA, USA, 2011.

(32) Lai, C. -Y.; Zhong, L.; Zhang, Y.; Chen, J. -X.; Wen, L. -L.; Shi, L. -D.; Sun, Y. -P.; Ma, F.; Rittmann, B. E.; Zhou, C.; Tang, Y.; Zheng, P.; Zhao, H. -P. *Environ. Sci. Technol.* **2016**, *50*, 5832-5839.

(33) Mjos, K. D.; Orvig, C. *Chem. Rev.* **2014**, *114*, 4540-4563.

(34) Purvis, E. R. *J. Agric. Food Chem.* **1955**, *3* (8), 665.

(35) Marin, R.; Ahuja, Y.; Bose, R. N. *J. Am. Chem. Soc.* **2010**, *132*, 10617-10619.

(36) Toal, S. J.; Trogler, W. C. Luminiscent Silole Nanoparticles as Chemical Sensors for Carcinogenic Chromium (VI) and Arsenic (V). In *Nanotechnology and the Environmental;* American Chemical Society: Washington, DC, 2004, pp 169-172.

(37) Patil, M.; Sheth, K. A.; Krishnamurthy, A. C.; Devarbhavi, H. *J. Clin. Exp. Hetatol.* **2013**, *3* (4), 321-336.

(38) Wu, F.; Wang, J.; Pu, C.;Qiao, L.; Jiang, C. *Int. J. Mol. Sci.* **2015**, *16*, 6419-6432.

(39) Ding, X.; Xie, H.; Kang, J. *J. Nutr. Biochem.* **2011**, *22* (4), 301-310.

(40) Steinbach, J.; Anderson, C. J.; Mäcke, H. R. Copper-64 Radiopharmaceuticals for Receptor-Mediated Tumor Imaging and Radiotherapy. Ph.D. Technischen Universität Dresden, Alemania, 1979.

(41) Dermirbilek, M.; Piskin, E. *Hacettepe J. Biol. Chem.* **2008**, *36* (4), 263-271.

(42) Martín-Caballero, J.; Wéry, A. S. J.; Reinoso, S.; Artetxe, B.; San Felices, L.; Gutiérrez-Zorrilla, J. M. *Inorg. Chem*. **2016**, *55* (10), 4970-4979.

(43) Liang, X.; Sadler, P. J. *Chem. Soc. Rev.* **2014**, *33*, 246-266.

(44) Li, J.; Zhu, Y.; Hazeldine, S. T.; Firestine, S. M.; Oupicky, D. *Biomacromolecules*, **2012**, *13*, 3220-3227.

(45) Chen, D.; Cui, Q. C.; Yang, H.; Barrea, R. A.; Sarkar, F. H.; Sheng, S.; Yan, B.; Reddy, G.; Dou, Q. P. *Cancer Res.* **2007***, 67*, 1639-1647.

(46) Parker, L. L.; Lacy, S. M.; Farrugia, L. J.; Evans, C.; Robins, D. J.; O'Hare, C. C.; Hartley, J. A.; Jaffar, M.; Stratford, I. J. *J. Med. Chem.* **2004**, *47*, 5683-5689.

(47) Dolomanov, O. V.; Bourhis, L. J.; Gildea, R. J.; Howard, J. A. K.; Puschmann, H. *J. Appl. Crystallogr.* **2009**, *42*, 339.

(48) Sheldrick, G. M. *Acta Crystallogr.* **2008**, *A64*, 112.

(49) Macrae,C. F.; Bruno, I. J.; Chisholm, J. A.; Edgington, P. R.; McCabe, P.; Pidcock, E.; Rodriguez-Monge, L.; Taylor, R.; Van de Streek, J.; Wood, P. A. *J. Appl. Crystallogr.* **2008**, *41*, 466.

(50) Spek, A. L. *Acta Crystallogr.* **2009**, *D65*, 148.

(51) Nakamoto, K. Inorganic Compounds. In *Infrared and Raman Spectra of Inorganic and Coordination Compounds;* Wiley: New York, 1986, pp 101-190.

(52) Babushkine, O.; Voyiatzis, G.; Ostvold, T. *Acta Chem. Scand.* **1999**, *53*, 320-328.

(53) Diaz, G.; Clavijo, R. E.; Campos-Vallette, M. M.; Saavedra, M.; Diez, S.; Muñoz, R. *Vib. Spectrosc.* **1997**, *15*, 301-209.

(54) Golcu, A.; Tümer, M. *Inorg. Chim. Acta* **2005**, *358*, 1785-1797.

(55) Fortes, A. D.; Wood, I. G. *Powder Diffr.* [Online] **2012**, *27*.

(56) Fortes, A. D. *Acta Crystallogr E Crystallogr Commun*. **2015**, *71*, 592–596.

(57) Pérez-Toro, I.; Domínguez-Martín, A.; Choquesillo-Lazarte, D.; Vílchez-Rodríguez, E.; González-Pérez, J. M.; Castiñeiras, A.; Niclós-Gutiérrez, J. *J. Inorg. Chem.* **2015**, *148*, 84-92.

(58) Fidalgo, A. MOFs basados en metaloporfinas: diseño estructural orientado a la biomimetización de sus propiedades naturales. Ph.D. Universidad del País Vasco, UPV/EHU, Leioa, Spain, 2014.

(59) Alvarez, S.; Avnir, D.; Llunell, M.; Pinsky, M. *New J. Chem.* **2002**, *26*, 996-1009.